



UiT The Arctic University of Norway

Faculty of Biosciences, Fisheries and Economics

Department of Arctic and Marine Biology

Historic changes in abundance, biomass and taxonomic composition of seaweed-associated fauna in Kongsfjorden, Svalbard

Jessica Niklass

BIO-3950 Master's thesis in Biology, November 2022

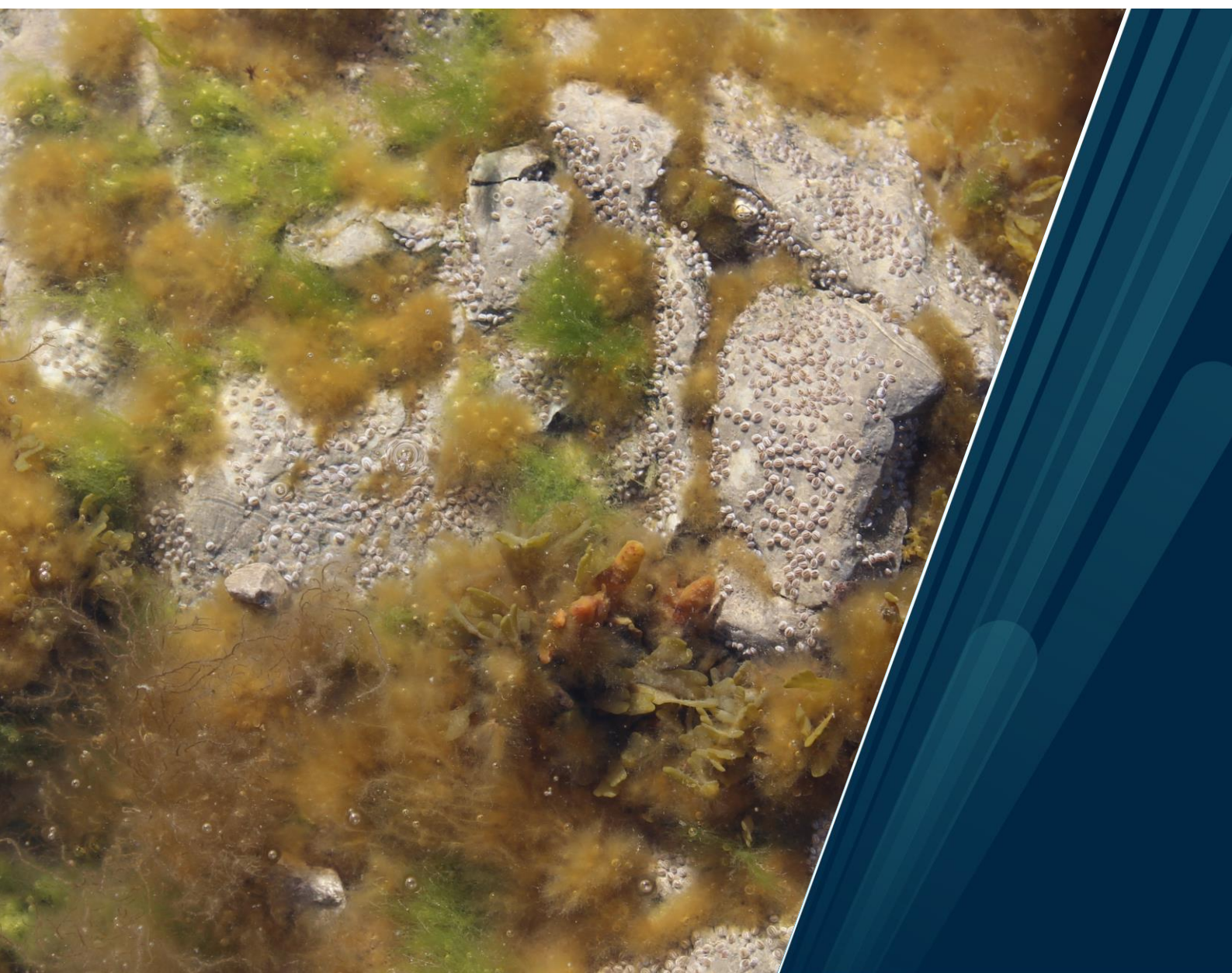


Table of Contents

Acknowledgements	1
Abstract	2
1 Introduction	3
1.1 Climate change in the Arctic	3
1.2 Seaweed ecosystem	4
1.3 Observed trends in Kongsfjorden	5
1.4 Study aim.....	6
2 Material and Methods.....	8
2.1 Study Site.....	8
2.2 Sampling.....	9
2.3 Statistical Analysis	12
3 Results	15
3.1 Total abundance.....	15
3.2 Total biomass.....	17
3.3 Taxonomic composition	19
4 Discussion	22
4.1 Summary of Results.....	22
4.2 Seaweed as ecosystem engineer	22
4.3 Disturbance through ice scouring	23
4.4 Changes in taxonomic composition.....	24
4.4.1 Contrary trends in suspension feeder biomass	25
4.5 Food web interactions.....	27
4.6 Future outlook.....	27
4.7 Conclusion.....	28
References	29
Appendix	36

List of Figures

Fig. 1 Location of study site. A Map of Svalbard. Kongsfjorden is marked with a box. B Map of Kongsfjorden. The study site, Hansneset, is marked with a cross. (Maps modified from Norwegian Polar Institute; retrieved from https://geokart.npolar.no/Html5Viewer/index.html?viewer=Svalbardkartet on 23 February 2022).....	8
Fig. 2 Sampling quadrat. Subsample a, macroalgae encased in a mesh bag, covered an area of 50 x 50 cm (area a+b). Subsample b, macrofauna attached to the bottom, covered an area of 25 x 25 cm (area b). Kelps and sea urchins were collected from the entire 1 m ²	9
Fig. 3 Most fauna was attached to the holdfast while the blade was often bare.	10
Fig. 4 Spirorbidae, small annelid worms in calcareous tubes, attached to algae (picture taken in Tromsø).....	10
Fig. 5 Individuals were sorted into aluminum dishes by taxa before weighing.....	11
Fig. 6 All organic matter was burned in the muffle furnace. Only the empty shells remained.	11
Fig. 7 Total abundance (individuals m ⁻²) at each sampling depth and year. The line inside a box indicates the median and the cross indicates the mean. The box marks the first and third quartile. The whiskers include the maximum and minimum values. The horizontal line across each plot shows the average total abundance from all depths of each year.	15
Fig. 8 Direction and size of temporal and depth effects on total abundance. Squares and whiskers mark mean and 95% confidence interval (CI) of effect sizes as log ratio of total abundance. The column at the right side lists the exact mean effect size and 95% CI. The size of squares is proportional to the precision of the estimate, with larger symbols indicating higher precision. The dotted line indicates no difference in total abundance between compared measurements. Negative and positive values indicate de- and increase in total abundance, respectively, between compared years or depths. A Effect of year: Total abundance of each sampling year, including all depths, was compared with the other years. B Effect of depth: Total abundance at each depth, averaged over all years, was compared with the other depths. C Interactive effect of year and depth: Each depth was compared with the same depth of another sampling year.	16
Fig. 9 Total biomass as ash-free dry weight (g m ⁻²) at each sampling depth and year. The line inside a box indicates the median and the cross indicates the mean. The box marks the first	

and third quartile. The whiskers include the maximum and minimum values. The horizontal line across each plot shows the average total abundance from all depths of each year. 17

Fig. 10 Direction and size of temporal and depth effects on total biomass. Squares and whiskers mark mean and 95% confidence interval (CI) of effect sizes as log ratio of total biomass. The column at the right side lists the exact mean effect size and 95% CI. The size of squares is proportional to the precision of the estimate, with larger symbols indicating higher precision. The dotted line indicates no difference in total biomass between compared measurements. Negative and positive values indicate de- and increase in total biomass, respectively, between compared years or depths. **A** Effect of year: Total biomass of each sampling year, averaged over all depths, was compared with the other years. **B** Effect of depth: Total biomass at each depth, considering all years, was compared with the other depths. **C** Interactive effect of year and depth: Each depth was compared with the same depth of another sampling year. 18

Fig. 11 Average biomass as ash-free dry weight (g m^{-2}) at each sampling depth, and all depths combined (column labeled “all”), for each sampling year. Each color represents one taxonomic group. 20

Fig. 12 Principal component analysis showing the difference in taxonomic composition for all combinations of years (color) and depths (symbols). The most influential taxa (arrows) revealed by SIMPER analysis are Ascidiacea (Asc), Bryozoa (Bry), Cirripedia (Cir), and Echinoidae (Ech). The orientation and length of the arrows represents to which principal component (PC) the taxon contributes the most and how strong. The ellipses depict the 95% confidence interval for each year. 21

Acknowledgements

I would like to express my thanks to my supervisors, particularly my main supervisor Markus Molis (University of Tromsø), but also Christian Buschbaum (Alfred Wegener Institute Sylt) and Paul Renaud (Akvaplan-niva) for their support and guidance. I am grateful to the AWI dive team led by Markus Brand for collecting the samples, and to the AWIPEV station leader and staff organizing my stay in Ny Ålesund. I also had great pleasure working with Simon Jungblut (University of Bremen), and the algae team from AWI Bremen, including Luisa Düsedau and Inka Bartsch. I would like to thank Markus Paar (University of Rostock) and Haakon Hop (Norwegian Polar Institute) for providing the data from previous sampling campaigns.

The thesis fieldwork was funded through the Arctic Field Grant by the Research Council of Norway (Project number: 322273). Thanks should also go to AWI for covering the costs of travel and accommodation of my supervisor Markus Molis.

This thesis was conducted in the frame of the project FACE-IT (The Future of Arctic Coastal Ecosystems – Identifying Transitions in Fjord Systems and Adjacent Coastal Areas). FACE-IT has received funding from the European Union's Horizon 2020 research and innovation programme under grant agreement No 869154.

Abstract

The Arctic is warming rapidly. Atmospheric temperatures in the Barents Sea region are increasing 5 – 7 times faster than the global average. As a result, Arctic sea ice extent is declining by nearly 12% per decade during the summer months. The study site in Kongsfjorden, Svalbard, has been mostly ice free since 2006. These changes in the physical environment likely affect the ecology of coastal Arctic ecosystems. Increased underwater irradiance seems to improve the growth of kelp forests on rock shores. This thesis is a continuation of a time series to estimate historic developments in abundance, biomass, and taxonomic composition of seaweed-associated fauna, comparing data from 2021 with data from 2012/13 and 1996/98. At each time point, samples were collected along the same gradient from 2.5 m to 15 m water depth. There is limited evidence for a difference in taxonomic composition between 2021 and 2012/13, while taxonomic composition in 1996/98 was significantly different from both other time points. Moreover, both faunal abundance and biomass increased about two-fold between 2012/13 and 2021. These results might suggest that the seaweed-associated fauna at Hansneset reached a new stable state after initial shifts in the taxonomic composition between 1996/98 and 2012/13. Differences in taxonomic composition, based on biomass data, were largely a result of an increase in cirripedian and decrease in bryozoan biomass. These taxonomic groups possibly show different responses to some biotic and abiotic factors, such as macroalgae cover or sedimentation.

1 Introduction

1.1 Climate change in the Arctic

The impacts of climate change are especially strong in the Arctic. The strongest warming is observed in the Barents Sea region where surface air temperatures have been increasing 5 – 7 times faster than the global average (Isaksen et al., 2022). While the temperature increase occurs in all seasons, it is considerably greater during winter than during summer. Winter air temperatures in Svalbard increased by 3.4 – 4.6 °C in recent decades. This strong warming is mainly driven by sea ice decline, higher sea surface temperatures, and a general background warming (Isaksen et al., 2016). The annual mean air temperature in Svalbard is predicted to increase by 3 – 10 °C towards the end of the 21st century, two to three times higher than the estimated global average increase in air temperature under the same emission scenarios (Hanssen-Bauer et al., 2019). Water temperatures around Svalbard have been increasing as well, due to changes in atmospheric circulation patterns bringing more warm Atlantic Water from the West Spitsbergen Current (WSC) into the fjords on the westside of Svalbard, where water temperatures are increasing by up to 2 °C per decade (Cottier et al., 2007; Orr et al., 2019). These changes in the abiotic environment influence the local ecosystems. The warming leads to an atlantification of Arctic communities as distribution ranges of Atlantic species, such as the blue mussel *Mytilus edulis*, shift northwards (Berge et al., 2005; Polyakov et al., 2020).

As a result of the warming, sea ice extent in the Arctic has been declining by nearly 12% per decade in September and 3% per decade in March (Hanssen-Bauer et al., 2019). At the same time, the sea ice is getting thinner as multi-year ice is increasingly getting replaced by first-year ice. The Arctic Ocean is expected to be only seasonally ice-covered by the middle of this century (Notz & Stroeve, 2016). Around Svalbard, the most pronounced sea ice loss occurs during the winter months, as fjords on the west coast of Svalbard are ice-free during summer (Muckenhuber et al., 2016; Onarheim et al., 2018). Sea ice scouring in Svalbard fjords can occur frequently down to a depth of 4.5 m (Hop et al., 2012), reducing both benthic abundance and biomass. Recovery usually takes several years due to the slow rates of growth and reproduction of Arctic benthos (Molis et al., 2019). Thus, sea ice loss may be beneficial for the macrobenthos in the intertidal zone due to less disturbance through ice scouring.

Furthermore, increasing precipitation and glacier melt in Svalbard lead to higher runoff (Schuler et al., 2020). The modelled net mass balance of Svalbard glaciers of -8.7 Gt/year is predicted to become even more negative in the future (Aas et al., 2016). The temperature of near-surface layers of the permafrost in Svalbard has been continuously increasing (Hanssen-Bauer et al., 2019). The permafrost in Svalbard is sensitive to warming due to its relatively high temperature, especially close to the shoreline, where coastal erosion can occur. Increased runoff and coastal erosion lead to greater sediment input into the fjords (Fritz et al., 2017).

Both sediment and sea ice cover attenuate the irradiance in the water. High run-off in combination with phytoplankton blooms increases the turbidity during summer, while the water is still clear in spring (Bartsch et al., 2016; Sukhanova et al., 2009). Moreover, sea ice and snow can reduce the underwater irradiance greatly due to low transmittance.

Photosynthetically active radiation (PAR) below a 1 m thick ice cover can be reduced to 8.5% compared to the air above (Hanelt et al., 2001). A lack of sea ice therefore increases the annual light availability for marine algae and the length of the productive season (Clark et al., 2013). While high turbidity in glacier discharge areas may inhibit seaweed growth, overall trends seem to be positive with seaweed biomass increasing across the Arctic. With continued sea ice loss, seaweeds are expected to become more abundant along the Arctic coastline (Krause-Jensen et al., 2020; Scherrer et al., 2019). An increase in macroalgae cover has already been observed in Svalbard (Kortsch et al., 2012).

1.2 Seaweed ecosystem

Seaweeds (or macroalgae) are highly productive primary producers and hotspots for biodiversity (Charpy-Roubaud & Sournia, 1990; Miller et al., 2018). They are defined as macroscopic, multicellular, marine algae that can be distinguished into three groups: green algae (Chlorophyta), brown algae (Phaeophyceae), and red algae (Rhodophyta; (Lobban & Harrison, 1994). Kelps, brown algae of the order Laminariales, form large individuals often dominating biomass on rocky shores. In Kongsfjorden, red algae are found in the understory of kelp forests and dominate the vegetation below the depth extent of kelps around 10 – 15 m (Hop et al., 2012).

Seaweeds increase the local biodiversity and abundance of many invertebrate species, which often exceed 100 000 ind. m⁻² in macroalgae beds along the coast of Norway (Christie et al.,

2009), through facilitation, i.e., an interaction that benefits at least one of the species and causes harm to neither. Facilitation includes associational defences by removing competitors or deterring predators, and the amelioration of environmental stress, e.g. an intertidal seaweed canopy reducing thermal and desiccation stress allowing the distribution of many organisms to extent into areas where they could not survive without benefactors (Bruno et al., 2003). As ecosystem engineers that heavily modify their habitat, seaweeds may facilitate associated fauna simply through their presence, as they provide shelter from predation, substrate for sessile species, and food (Schultze et al., 1990; Wright et al., 2014). Invertebrates in return may facilitate seaweeds through excretion of nitrogen, promoting algae growth (Bracken et al., 2007).

Kelps increase the habitat complexity due to their structure that consists of the leaf-like blade, the holdfast used to attach an individual to the seafloor, and the stipe connecting blade and holdfast. While the blade regrows yearly, the holdfast and stipe are perennial (Lobban & Harrison, 1994). Due to its longevity and structure, holdfasts house the highest abundance of associated fauna, with less mobile species than on seasonal algae (Norderhaug et al., 2002; Shunatova et al., 2018).

Primary production of seaweeds may exceed marine phytoplankton primary production up to ten times (Charpy-Roubaud & Sournia, 1990) making seaweeds a valuable food source not only for grazers, such as sea urchins or gastropods, but also for detritivores, like amphipods, which feed on degraded seaweed biomass (Norderhaug et al., 2003). Herbivores are estimated to reduce abundance of marine benthic primary producers by 68% on average, which is consistently higher than estimates from terrestrial systems (Poore et al., 2012). In return, species from higher trophic levels, such as fishes and birds, forage on seaweed-associated fauna (Fredriksen, 2003).

1.3 Observed trends in Kongsfjorden

When a system changes from one stable state to another after a period of gradual change, such as the sudden shift of the rocky bottom communities from predominantly calcareous algae to seaweeds after gradual temperature increase observed in two Svalbard fjords in the 1990s, it is called a tipping point (Kortsch et al., 2012). The winter 2005/06 is considered a tipping point for Kongsfjorden, a fjord located on the west coast of Svalbard (Fig. 1 A). That winter,

upwelling along the western shelf of Svalbard caused a strong inflow of Atlantic water from the WSC into Kongsfjorden (Cottier et al., 2007). The warm water restricted sea ice formation to the inner part of Kongsfjorden. In contrast to previous winters, where sea ice covered the entire fjord, maximum sea ice extent in winter did not cover the entire fjord from 2006 onwards, except for February 2011 (Pavlova et al., 2019).

Bartsch et al. (2016) and Paar et al. (2016) investigated changes of seaweeds and their associated fauna along a depth gradient down to 15 m depth in Kongsfjorden between 1996/98 and 2012/13, i.e. before and after the putative tipping point. Seaweed biomass was higher in 2012/13 than in 1996/98. The biomass peak shifted upwards from 5 m to 2.5 m depth due to an 8.2-fold increase in kelp biomass at 2.5 m. Likewise, the lower depth limit of most biomass-dominant kelps moved several meters up. These changes were attributed to sea ice loss and increased sedimentation (Bartsch et al., 2016). The depth distribution of the seaweed-associated fauna changed between 1996/98 and 2012/13, as well. Biomass at 2.5 m increased 10-fold, mostly due to sessile suspension feeders, such as Bryozoa, who benefit of the accumulation of detritus under the dense kelp canopy. Meanwhile, biomass at 15 m decreased greatly, mainly because of a reduction in mobile crustaceans and echinoderms, which were distributed more evenly at all sampled depths. The changes in faunal depth distribution seem to match with the trends observed in seaweed distribution (Paar et al., 2016).

1.4 Study aim

Abundance and biomass of the seaweed-associated fauna in Kongsfjorden before the putative tipping point in 2006 and 6 years later have been recorded previously (Paar et al., 2016). However, polar benthic organisms have low rates of growth, reproduction, and colonization compared to organisms at lower latitudes (Barnes & Conlan, 2007). The recovery of Arctic benthic communities after a disturbance can take over a decade (Beuchel & Gulliksen, 2008). Changes in species composition and succession induced by altered environmental conditions since 2006 might not have been completed within the relatively small timeframe of 6 years, i.e. between 2006 and the last benthic survey in 2013 by (Paar et al., 2016). Moreover, the community structure of the hard-bottom benthos in Kongsfjorden is correlated with the temperature of the WSC (Beuchel et al., 2006). The increasing water temperatures in Svalbard fjords may affect the seaweed-associated fauna directly or indirectly through modified habitat

availability (Bloskhina et al., 2021; Ørberg et al., 2018). Therefore, the study site was revisited in 2021 to continue the dataset on abundance and biomass of seaweed-associated fauna and investigate whether the magnitude and direction of previously observed trends in abundance, biomass and taxonomic composition of the seaweed-associated fauna continued or shifted. Differences between 2021 and the previous sampling campaigns are expected, because continued changes of environmental conditions are observed in Svalbard fjords (Hanssen-Bauer et al., 2019). However, there might be a smaller difference between the data from 2021 and 2012/13 than between 2012/13 and 1996/98, since a major shift in environmental conditions, i.e. from ice-covered to ice-free winters, occurred already between the first two sampling campaigns. Hence, recent changes (2013 to 2021) in traits of the seaweed-associated fauna are predicted to be of different magnitude than changes that were observed between earlier surveys (1996/98 to 2012/13). The changes are likely to be of different magnitude or direction across the sampling depths, due to environmental gradients such as light or ice scouring.

2 Material and Methods

2.1 Study Site

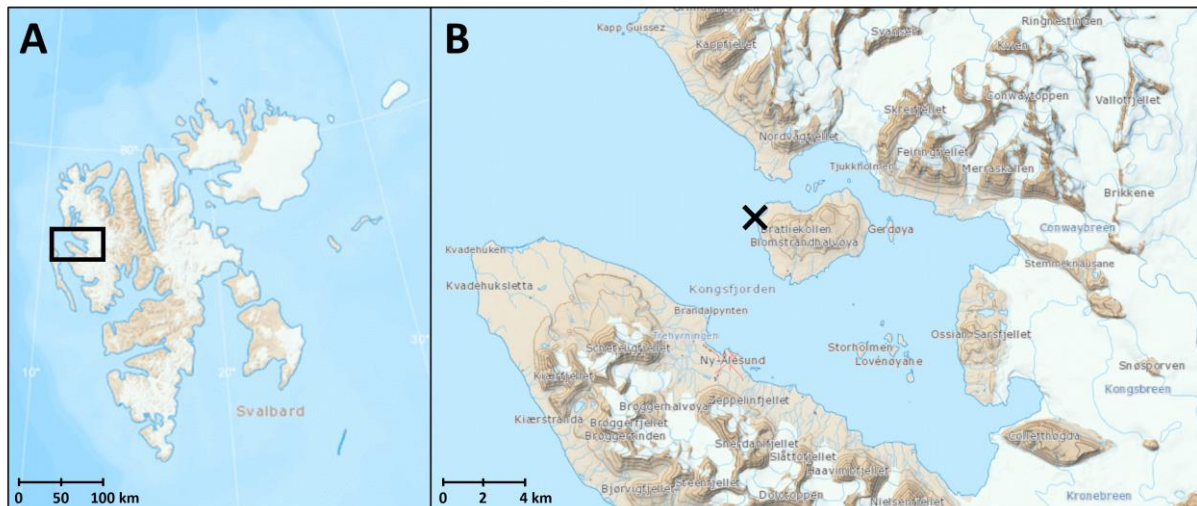


Fig. 1 Location of study site. **A** Map of Svalbard. Kongsfjorden is marked with a box. **B** Map of Kongsfjorden. The study site, Hansneset, is marked with a cross. (Maps modified from Norwegian Polar Institute; retrieved from <https://geokart.npolar.no/Html5Viewer/index.html?viewer=Svalbardkartet> on 23 February 2022)

Samples were collected at Hansneset, Kongsfjorden, ($78^{\circ}59.101'N$, $11^{\circ}57.793'E$) and analysed in the close-by laboratory in Ny Ålesund during June and July 2021. Kongsfjorden is about 20 km long, 4 – 10 km wide, and its outer basins reach down to 430 m depth (Vorontkov et al., 2013). Hansneset lies on the west side of Blomstrandhalvøya, the biggest island in Kongsfjorden (Fig. 1 B). The steep bedrock at Hansneset is barely covered by sediments due to strong wave exposure (Vorontkov et al., 2013).

A submarine glacial trough connects Kongsfjorden and the West Spitsbergen Current (WSC) across the shelf, allowing relatively warm and saline water ($T = 1.0 - 7.0^{\circ}C$, $S = 34.7 - 34$) to enter the fjord (Cottier et al., 2005; Tverberg et al., 2019). Kongsfjorden has five tidewater glaciers. The release of freshwater, sediments, and icebergs from these glaciers possibly increased over the entire study period (from 1996 to 2021), due to the mass loss of Svalbard glaciers since the 1960s (Schuler et al., 2020). Additional freshwater input comes from snowmelt and rivers, but glaciers are the main source, as 80% of the drainage area in Kongsfjorden is covered by glaciers (Tverberg et al., 2019).

Decreasing extent of fast-ice in Kongsfjorden during the observation period 2003 – 2016 was described by (Pavlova et al., 2019). Prior to 2006, the entire fjord was ice-covered in all years. The maximum fast-ice cover was reached in the months January – March and ice break up

occurred in June. After 2006, relatively little ice cover was found in Kongsfjorden, while Hansneset was not ice-covered since 2006, with the exception in 2011. The first sampling campaign in 1996/98 and the third campaign in 2021 are not included in the observation period of sea ice extent by (Pavlova et al., 2019), however 1998 was a cold year (Maturilli et al., 2013) with a 1 m thick ice cover persisting until mid-June (Hanelt et al., 2001). Air temperature data, which have a strong influence on the fast-ice cover (Pavlova et al., 2019), are available for 2021 (Skålin et al., 2022). Based on the air temperature data from Ny-Ålesund and the previously described trend, it can be expected that Hansneset was not ice-covered in 2021.

A macroalgae belt covers the rocky sublittoral at Hansneset down to 30 m depth (Hop et al., 2012). The euphotic zone at Hansneset extended to 24 m in June and to 6 m in July 1997 (Bischof et al., 1998). Kelp species, such as *Alaria esculenta*, *Laminaria digitata*, and *Saccharina latissima*, dominate the shallow areas to around 10 m depth. Average kelp biomass at 2.5 m in 2012 was 14.4 kg m⁻². Below 15 m, near the depth limit of most kelps, dominate red algae. The most common species at 10 m and 15 m depth are *Ptilota* spp., *Phycodrys rubens*, and *Euthora cristata* (Bartsch et al., 2016). The dense kelp belt at 2.5 m – 5 m depth is largely inhabited by sessile suspension feeders, such as bryozoans, annelids, and bivalves. There are more mobile species, such as gastropods, echinoderms, and decapods at 10 m – 15 m compared to shallower depths. A large number of Cirripedia are found on the rocks beneath the seaweed (Paar et al., 2016).

2.2 Sampling

SCUBA divers collected macroalgae and all associated fauna (mobile and sessile) along a depth transect at 2.5 m, 5 m, 10 m, and 15 m. Four replicates of 1 m² quadrats were sampled at each depth. The position was determined before the dive by pulling a random number. In case the position landed on soft sediment, divers followed the transect to the next hard substrate area. Each replicate was separated by a minimum of 2 m. A steel frame of 1

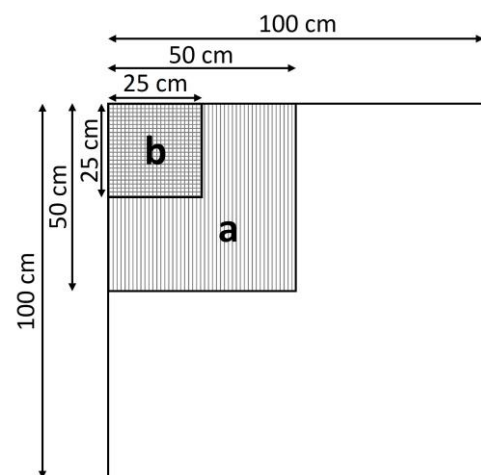


Fig. 2 Sampling quadrat. Subsample a, macroalgae encased in a mesh bag, covered an area of 50 x 50 cm (area a+b). Subsample b, macrofauna attached to the bottom, covered an area of 25 x 25 cm (area b). Kelps and sea urchins were collected from the entire 1 m².



Fig. 3 Most fauna was attached to the holdfast while the blade was often bare.

m² size with cord indicating subsample areas was used for marking the quadrat. The divers collected all kelps from the 1 m² quadrats. A 50 cm x 50 cm subsample of macroalgae and -fauna was enclosed in a mesh bag (1 mm mesh size) to retain mobile fauna (subsample a). All macrofauna directly attached to the seafloor in an area of 25 x 25 cm was removed with a diver's knife and put in a separate mesh bag (subsample b). All sea urchins inside the 1 m² quadrats were collected (Fig. 2). The samples were stored in flow-through tanks with ambient seawater in the Marine Laboratory in Ny Ålesund until further processing, usually within 24 h.



Fig. 4 *Spirorbidae*, small annelid worms in calcareous tubes, attached to algae (picture taken in Tromsø).

For separating fauna from the algae, all fauna was removed from the holdfast and blade with tweezers (Fig. 3). Afterwards the algae were rinsed with filtered seawater to wash out any missed animals, which were separated from the rinsing water with a 500 µm sieve. Animals collected from the algae and the sieve were stored in a container with filtered seawater until the fresh weight weighing step. Using dissecting-microscopes

(magnification: 6.4 – 40x), all animal individuals were

sorted into 19 different taxonomic groups, as in the previous survey in 2012/13 (Paar et al., 2016): Polychaeta, Ascidiacea, Bryozoa, Cirripedia, Amphipoda, Oregoniidae, Paguridae, Hippolytidae, Echinoidae, Ophiuroidea, Muricidae, Bivalvia, Buccinidae, Polyplacophora, Actinaria, Hydrozoa, Nemertea, Porifera, and Pycnogonida. This grouping was used for analysis of taxonomic composition. All individuals except of colonial taxa, such as Bryozoa, Hydrozoa or Porifera, were counted. In case of high numbers (i.e. hundreds) of *Spirorbidae* (Fig. 4) on kelp blades, one person estimated the number. The person would always be the same to ensure comparability between samples. Due to tremendously high number of *Spirorbidae* on red algae, *Spirorbidae* individuals were counted on only part of the algae found in a sample. Subsequently, the fresh weight of both, the red algae of which *Spirorbidae* individuals had been counted and the remaining red algae of which *Spirorbidae* individuals

had not been counted were weighed (precision: 0.01 g) to estimate the total Spirorbidae abundance of the sample using the following formula.

$$S_a = \frac{S_c}{A_c} * (A_c + A_n) \quad (1)$$

S_a : all Spirorbidae

S_c : counted Spirorbidae

A_c : fresh weight of algae on which Spirorbidae were counted [g]

A_n : fresh weight of algae on which Spirorbidae were not counted [g]



Fig. 5 Individuals were sorted into aluminum dishes by taxa before weighing



Fig. 6 All organic matter was burned in the muffle furnace. Only the empty shells remained.

5After counting, all animals were dried with paper towels and put into weighed aluminium dishes sorted by taxon (Fig. 5). Fresh weight was determined with a micro scale (Sartorius Analytic A 120 S, precision: 0.1 mg). Afterwards, samples were dried in a drying oven at 60 °C until weight constancy (min. 24 h). Because the dried animals take up water from the colder air as they are removed from the drying oven, all dishes were weighed twice, the second time in the opposite order of the first round. Then the mean for each taxon was calculated. This way the mean time outside of the drying oven should be about the same for each taxon, thus method-derived differences in dry mass among taxa due to the uptake of water from the air was minimised. Thereafter all organic material in the samples was burned in a muffle furnace (Nabertherm B180) that was heated to 450 °C within 2 h and remained at 450 °C for 4 h before cooling down (Fig. 6). The remaining ash was weighed with the same procedure as dry weight. To calculate ash-free dry weight (AFDW), ash weight was subtracted from dry weight. AFDW is a measure for all organic matter in the sample and was used in the statistical analysis.

2.3 Statistical Analysis

The data collected as described above was compared to data from 2012/13 (Paar et al., 2016) and 1996/98 (Voronkov et al., 2013) to investigate historic changes. As a balanced design with equal number of observations is preferable due to higher statistical power (Shaw & Mitchell-Olds, 1993), only data of 2013 were used for the analysis of biomass. The sample size for both 2012 and 2013 combined ($n = 9$) would be more than two times higher than the sample size in 2021 ($n = 4$). The sample size in 2013 was identical with 2021, but higher in 2012 ($n = 5$). For the analyses of abundance data, however, 2012 data was chosen due to differences in the sampling method in 2013. In contrast to 2012 and 2021, algae were not enclosed in a mesh bag in 2013, resulting in a loss of small, fast-swimming fauna, which could affect estimates of abundance, but has negligible effects on biomass estimates. The difference in methods is expected to have a stronger impact on analysis results than the small difference in sample size. For the survey in 1996/98, data of both sampling years were used due to low sample size ($n = 2$). Both abundance and biomass data were standardised to 1 m^2 to compare between the different studies. All statistical analysis was performed in RStudio (RStudio Team, 2021).

Differences in faunal abundance and biomass were separately tested between sampling years and depths by one-way analysis of variance (ANOVA). A two-way ANOVA was used to test for an interactive effect of year and depth on abundance and biomass. The ANOVAs were followed by Tukey HSD post-hoc tests to investigate which sampling years or depths were different from each other. Homogeneity of variances was confirmed with Levene's test. If homogeneity of variances was not given, the level of significance was reduced from 0.05 to 0.01, lowering the probability of type I error (Ieno & Zuur, 2015). In these cases, the p-value will be written in *italics*. Normality could not be confirmed by Shapiro-Wilk test due to small sample size. To compare the magnitude and direction of the differences in abundance and biomass between studies, effect sizes were determined using the *escalc* function of the *metafor* package and were visualised as forest plots (e.g. Fig. 8; Durlak, 2009; Viechtbauer, 2010). The response ratio (RR), the natural-log proportional change in the means (X) of two measurements to be compared, e.g. biomass at 2.5 m in 1996/98 vs. biomass at 2.5 m in 2021, and its variance (σ^2) were calculated with the following formulas (Hedges et al., 1999; Lajeunesse, 2011).

$$RR = \ln \left(\frac{X_1}{X_2} \right) \quad (2)$$

$$\sigma^2(RR) = \frac{(SD_1)^2}{N_1 X_1^2} + \frac{(SD_2)^2}{N_2 X_2^2} \quad (3)$$

RR: Response ratio

X: Mean

$\sigma^2(RR)$: Variance of response ratio

SD: Standard deviation

N: Sample size

This results in relative values, that can easily be compared across studies and are symmetric around 0. Positive values indicate an increase, negative values indicate a decrease. As a general rule effect sizes of 0.20 can be considered small, 0.50 medium, and 0.80 large (Durlak, 2009).

Furthermore, differences in taxonomic composition over depth and time was analysed by permutational multivariate analysis of variance (PERMANOVA; using 99999 permutations) based on Bray-Curtis dissimilarity, using the *adonis* function of the package *vegan* (Anderson, 2017). The results shown are based on biomass data, which is a better measure for productivity than abundance, since the size of an individual can influence its role in the ecosystem. PERMANOVA results based on abundance data were similar to biomass-based results (Tab. A1). Relative values i.e., the proportion of the taxa from the total biomass at each depth and in each year, were used for the multivariate analysis because Bray-Curtis dissimilarity based on relative values of a response variable (here biomass) includes both compositional differences and differences in absolute values (Greenacre, 2017). The absolute biomass values, however, were analysed with univariate methods as described above. The PERMANOVA was followed by pairwise comparisons, using the package *pairwiseAdonis* (Martinez Arbizu & Monteux, 2017), to determine which years and depths contributed to the differences found with PERMANOVA. Additionally, the function *simper* of the package *vegan* (Oksanen et al., 2020) was used to determine the relative contribution of taxa to the differences between groups up to a threshold of 50% (Clarke & Ainsworth, 1993). To visualize differences in taxonomic composition, a principal component analysis (PCA) was computed using the *prcomp* function of the package *stats* (R Core Team, 2021). The first two principal components (PC), which account for the largest part of the variation in the data, were plotted. Variables close to the center of the plot are less important for PC1 and PC2 (Abdi & Williams, 2010). The taxa with the strongest influence on taxonomic composition

revealed by simpler analysis were plotted as loading vectors, the orientation and length of the vector representing to which PC the taxon contributes the most and how strong (Hartmann et al., 2018).

3 Results

3.1 Total abundance

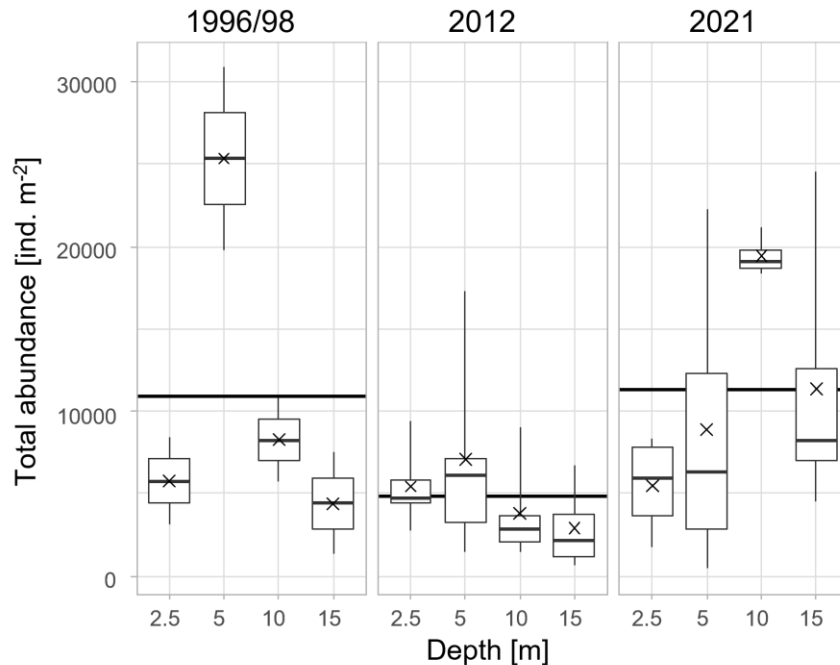


Fig. 7 Total abundance (individuals m^{-2}) at each sampling depth and year. The line inside a box indicates the median and the cross indicates the mean. The box marks the first and third quartile. The whiskers include the maximum and minimum values. The horizontal line across each plot shows the average total abundance from all depths of each year.

Total abundance of seaweed-associated fauna was highest in 2021, with an average 11273 ± 5927 ind. m^{-2} , followed by 1996/98 and 2012, with an average 10942 ± 9718 and 4799 ± 1838 ind. m^{-2} , respectively. Despite total abundance in 2012 being only half of both other years (Fig. 7), these differences were not statistically significant when using one-way ANOVA ($F_{2,41} = 4.70$, $p = 0.014$; a critical p-value of 0.01 was used here because of heterogeneity in variances). Yet, response ratios (RR) indicate strong temporal changes in total abundance of the seaweed-associated fauna between 1996/98 and 2012, and between 2012 and 2021 (Fig. 8 A). Total abundance strongly declined between 1996/98 and 2012 (RR = -0.82 [95% CI: $-1.46 - -0.19$]), followed by a comparatively strong increase in total abundance until 2021 (RR = 0.85 [95% CI: $0.55 - 1.16$]), reaching a similar level as in 1996/98 (RR = 0.03 [95% CI: $-0.64 - 0.70$]).

Averaged over all years, total abundance was highest at 5 m depth with an average 13740 ± 10070 ind. m^{-2} and lowest at 2.5 m with an average 5569 ± 180 ind. m^{-2} . Even though total abundance at 2.5 m depth was less than half of 5 m, no statistically significant difference was found when using one-way ANOVA ($F_{3,40} = 1.61$, $p = 0.203$). Yet, response ratios indicate

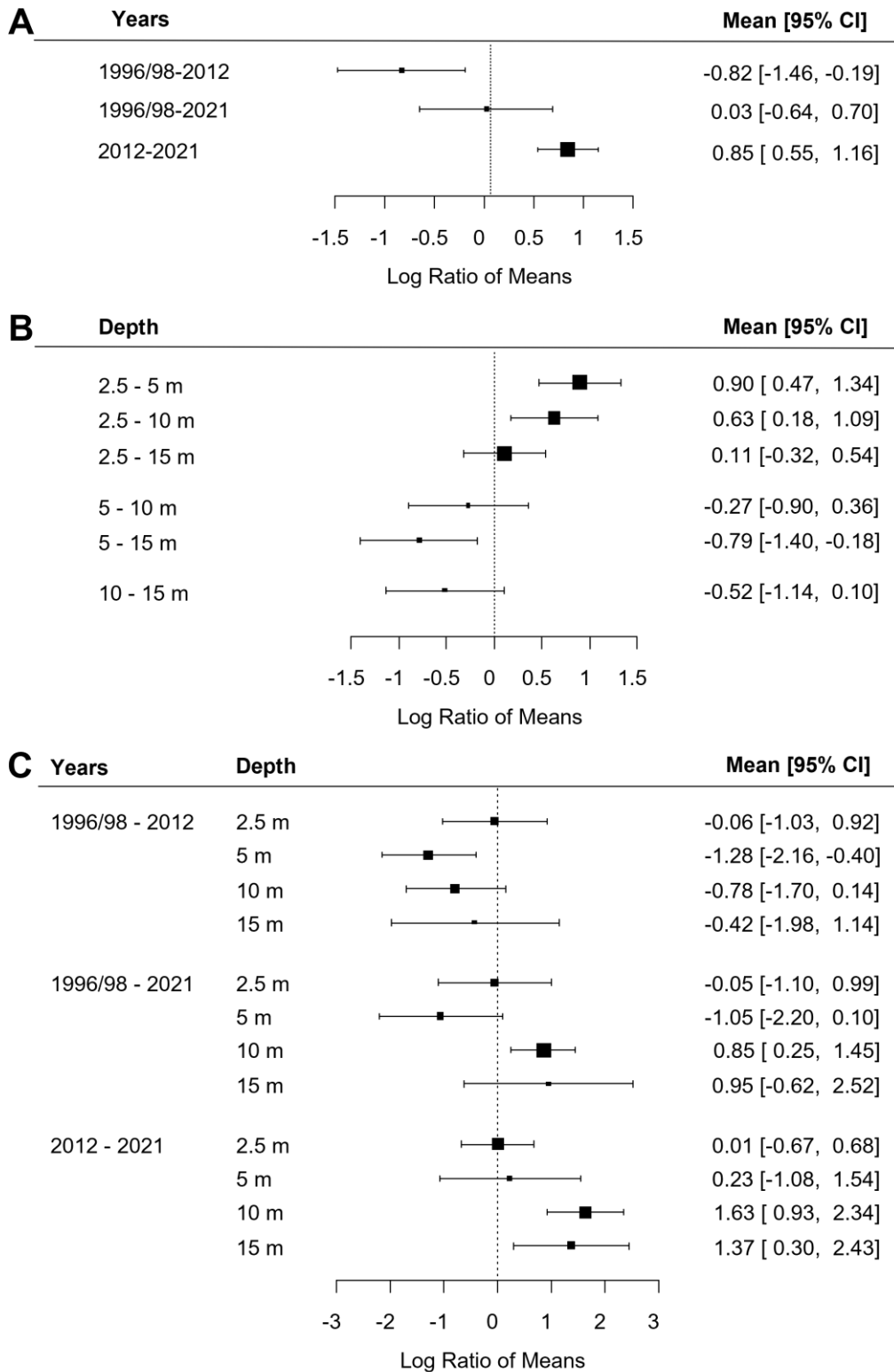


Fig. 8 Direction and size of temporal and depth effects on total abundance. Squares and whiskers mark mean and 95% confidence interval (CI) of effect sizes as log ratio of total abundance. The column at the right side lists the exact mean effect size and 95% CI. The size of squares is proportional to the precision of the estimate, with larger symbols indicating higher precision. The dotted line indicates no difference in total abundance between compared measurements. Negative and positive values indicate de- and increase in total abundance, respectively, between compared years or depths. **A** Effect of year: Total abundance of each sampling year, including all depths, was compared with the other years. **B** Effect of depth: Total abundance at each depth, averaged over all years, was compared with the other depths. **C** Interactive effect of year and depth: Each depth was compared with the same depth of another sampling year.

changes in total abundance with depth (Fig. 8 B). Total abundance strongly increased from 2.5 m to 5 m depth (RR = 0.90 [95% CI: 0.47 – 1.34]) and to 10 m to a lesser extent (RR = 0.63 [95% CI: 0.18 – 1.09]), followed by a strong decline from 5 m to 15 m depth (RR = -0.79 [95% CI: -1.40 – -0.18]).

In 2021 alone, total abundance was on average highest at 10 m depth with $19391 \pm 1248 \text{ ind. m}^{-2}$ and lowest at 2.5 m with $5480 \pm 3058 \text{ ind. m}^{-2}$. In both the previous studies, however, total abundance was highest at 5 m with $7056 \pm 6160 \text{ ind. m}^{-2}$ in 2012 and $25322 \pm 7860 \text{ ind. m}^{-2}$ in 1996/98 and lowest at 15 m depth with $2902 \pm 2443 \text{ ind. m}^{-2}$ and $4414 \pm 4364 \text{ ind. m}^{-2}$, respectively (Fig. 7). The statistically significant difference revealed by two-way ANOVA ($F_{6,32} = 4.69$, $p = 0.002$) is mostly a result of the decrease of total abundance at 5 m depth from 1996/98 to 2012 and the following increase at 10 m depth from 2012 to 2021. The interactive effect of time and depth explained 62.4% of the variance. The previously mentioned shift in the depth distribution of total abundance was reflected by large response ratios for the decrease at 5 m depth (RR = -1.28 [95% CI: -2.16 – -0.40]) and the increase at 10 m (RR = 1.63 [95% CI: 0.93 – 2.43]). Total abundance also increased strongly at 15 m depth between 2012 and 2021 (RR = 1.37 [95% CI: 0.30 – 2.43]; Fig. 8 C).

3.2 Total biomass

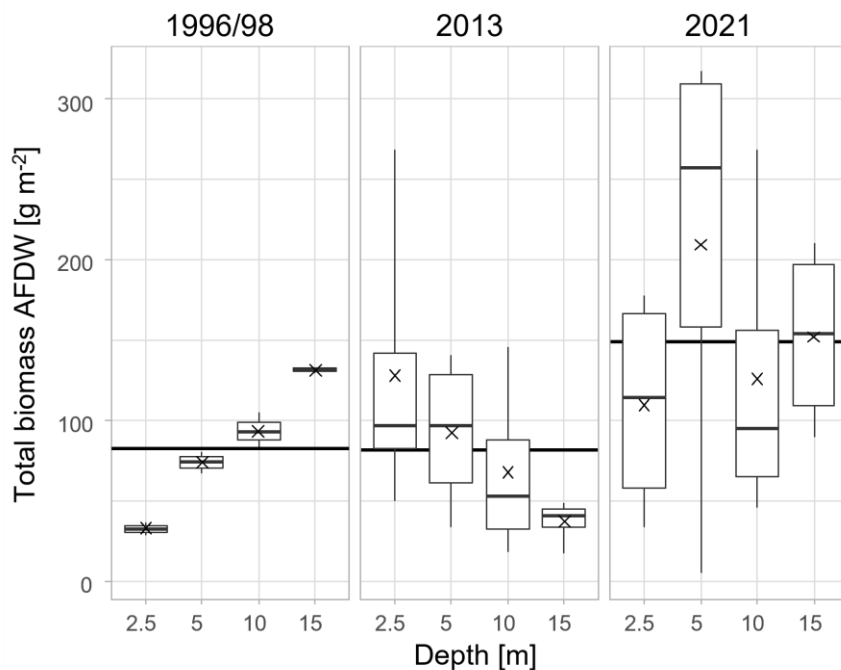


Fig. 9 Total biomass as ash-free dry weight (g m^{-2}) at each sampling depth and year. The line inside a box indicates the median and the cross indicates the mean. The box marks the first and third quartile. The whiskers include the maximum and minimum values. The horizontal line across each plot shows the average total abundance from all depths of each year.

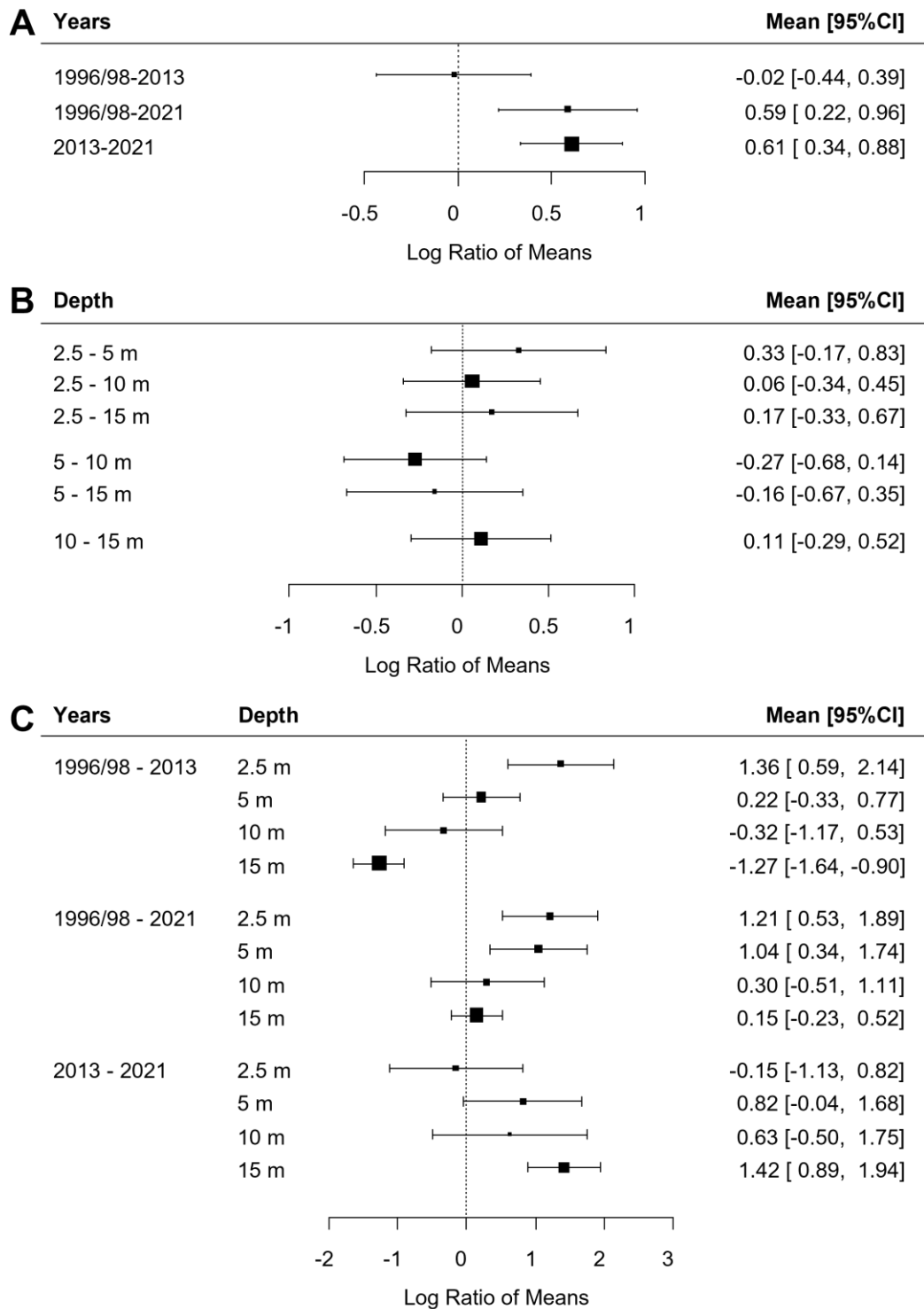


Fig. 10 Direction and size of temporal and depth effects on total biomass. Squares and whiskers mark mean and 95% confidence interval (CI) of effect sizes as log ratio of total biomass. The column at the right side lists the exact mean effect size and 95% CI. The size of squares is proportional to the precision of the estimate, with larger symbols indicating higher precision. The dotted line indicates no difference in total biomass between compared measurements. Negative and positive values indicate de- and increase in total biomass, respectively, between compared years or depths. **A** Effect of year: Total biomass of each sampling year, averaged over all depths, was compared with the other years. **B** Effect of depth: Total biomass at each depth, considering all years, was compared with the other depths. **C** Interactive effect of year and depth: Each depth was compared with the same depth of another sampling year.

Total biomass as ash-free dry weight of seaweed-associated fauna was highest in 2021 with an average $149.3 \pm 43.6 \text{ g m}^{-2}$, followed by 1996/98 and 2013, with an average of $82.8 \pm 41.0 \text{ g m}^{-2}$ and $81.2 \pm 38.6 \text{ g m}^{-2}$, respectively. Even though total biomass in 2021 was almost double of both other years (Fig. 9), these differences were not statistically significant when using one-way ANOVA ($F_{2,37} = 3.79$, $p = 0.032$). Response ratios, however, indicate temporal changes (Fig. 10 A), as total biomass increased between 2012 and 2021 (RR = 0.61 [95% CI: 0.34 – 0.88]).

Averaged over all years, total biomass was, like total abundance, highest at 5 m depth with an average $125.2 \pm 73.3 \text{ g m}^{-2}$ and lowest at 2.5 m depth with an average $90.2 \pm 50.6 \text{ g m}^{-2}$. The difference over depth is not significant (one-way ANOVA, $F_{3,36}=0.47$, $p=0.705$), matching with small response ratios for all comparisons between depths (Fig. 10 B).

In 2021 alone, total biomass was on average highest at 5 m depth with $209.2 \pm 144.8 \text{ g m}^{-2}$ and lowest at 2.5 m with $109.7 \pm 71.0 \text{ g m}^{-2}$, while in 2013 highest total biomass of $128.1 \pm 96.0 \text{ g m}^{-2}$ was at 2.5 m and continuously decreased with depth to $36.9 \pm 13.8 \text{ g m}^{-2}$ at 15 m. Contrary to 2013, in 1996/98 total biomass was lowest at 2.5 m with $32.7 \pm 5.9 \text{ g m}^{-2}$ and continuously increased with depth to $131.3 \pm 2.2 \text{ g m}^{-2}$ at 15 m. These differences were not statistically different when using two-way ANOVA ($F_{6,28} = 1.18$, $p = 0.347$). Nevertheless, large response ratios indicate strong differences in the depth distribution of total biomass over the study period (Fig. 10 C). In 2021, total biomass strongly increased at 5 m depth compared to 2013 (RR = 0.82 [95% CI: -0.04 – 1.68]) and 1996/98 (RR = 1.04 [95% CI: 0.34 – 1.74]). While total biomass at 15 m strongly decreased between 1996/98 and 2013 (RR = -1.27 [95% CI: -1.64 – -0.90]), it strongly increased again towards 2021 (RR = 1.42 [95% CI: 0.89 – 1.94]). Between 1996/98 and 2013 there was a strong decrease in total biomass at 2.5 m depth (RR = 1.36 [95% CI: 0.59 – 2.14]).

3.3 Taxonomic composition

The taxonomic composition of seaweed-associated fauna based on biomass data was significantly influenced by temporal effects (PERMANOVA, pseudo- $F_{2,28} = 6.25$, $p = 0.000$) which explained 18.7% of the variance. Specifically, 1996/98 was statistically different from 2021 (pairwise comparison, pseudo- $F_{1,22} = 9.15$, $p = 0.001$) and 2013 (pairwise comparison, pseudo- $F_{1,22} = 3.52$, $p = 0.043$; Fig. 12). The taxa with the highest influence on these

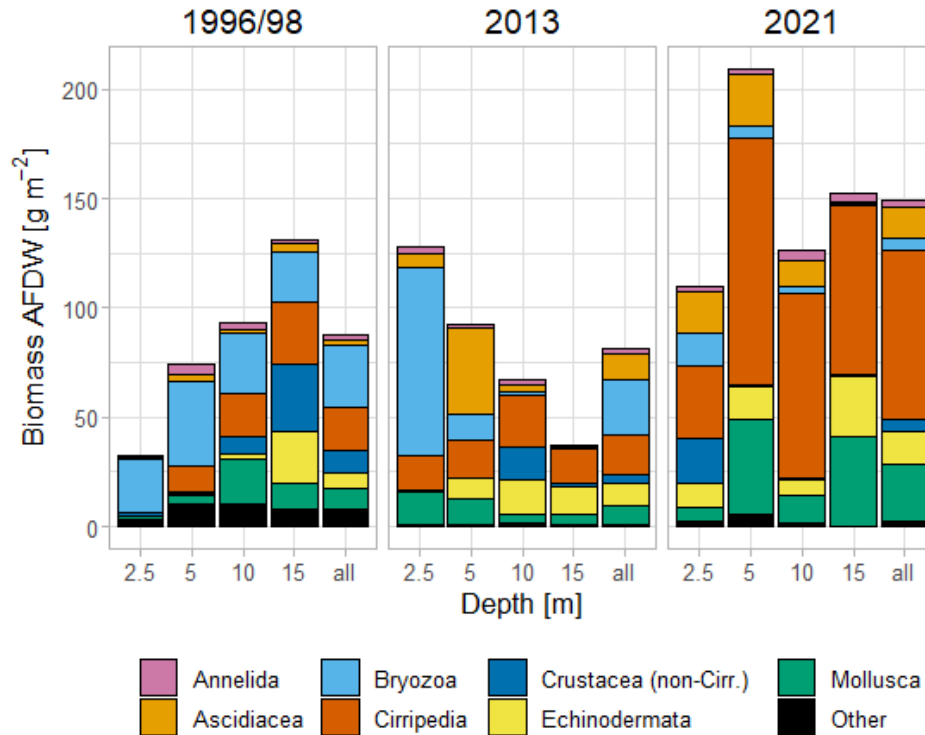


Fig. 11 Average biomass as ash-free dry weight ($g\ m^{-2}$) at each sampling depth, and all depths combined (column labeled "all"), for each sampling year. Each color represents one taxonomic group.

differences were Bryozoa (28.8%) and Cirripedia (26.2%) for the difference between 1996/98 and 2021, and again Bryozoa (27.7%) and Cirripedia (16.3%) but also Echinoidae (10.4%) for the difference between 1996/98 and 2013 (Fig. 12). Bryozoan biomass strongly declined after 2013 and contributed only 3.9% to the total biomass in 2021, averaged over all depths, while it was 32.4% in 1996/98 and 31.2% in 2013. In contrast, Cirripedia biomass strongly increased after 2013 contributing 51.6% to the total biomass in 2021. Cirripedia biomass was 22.6% in 1996/98 and 22.0% in 2013. The relative biomass of Echinodermata increased from 7.7% in 1996/98 to 12.0% in 2013 (Fig. 11).

Moreover, depth significantly affected taxonomic composition (PERMANOVA, pseudo- $F_{3,28} = 5.66$, $p = 0.000$), which explained 25.3% of the variance. Particularly, at shallower depths (2.5 m and 5 m) taxon composition was different from the deeper ones (10 m and 15 m). The difference between 2.5 m and 10 m (pairwise comparison, pseudo- $F_{1,22} = 5.84$, $p = 0.016$) and between 2.5 m and 15 m depth (pairwise comparison, pseudo- $F_{1,22} = 10.64$, $p = 0.000$) was mostly due to Bryozoa (32.2%; 31.7%) and Cirripedia (23.8%; 21.7%). The difference between 5 m and 15 m depth (pairwise comparison, pseudo- $F_{1,22} = 3.23$, $p = 0.049$) was mostly influenced by Cirripedia (19.7%), Ascidiacea (15.6%), Echinoidae (13.5%) and Bryozoa (12.7%; Fig. 12). No significant interactive effect of year and depth was found (PERMANOVA, pseudo- $F_{6,28} = 1.57$, $p = 0.059$).

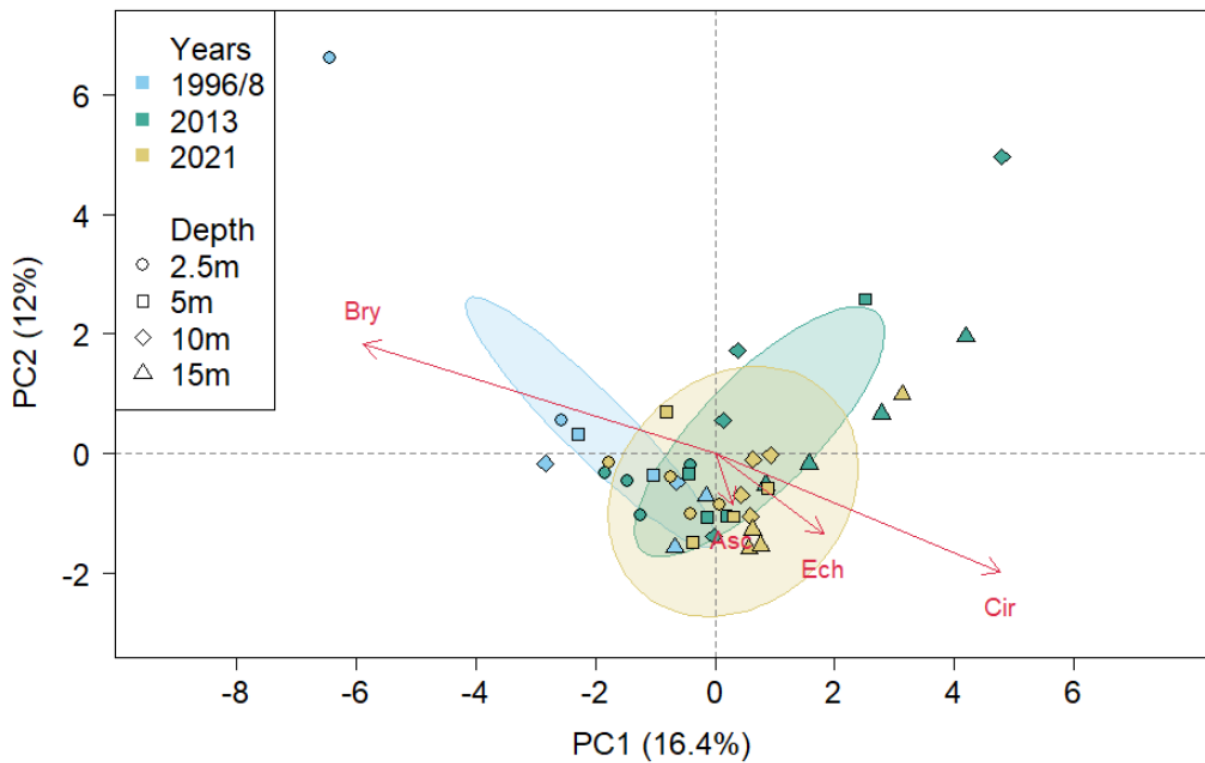


Fig. 12 Principal component analysis showing the difference in taxonomic composition for all combinations of years (color) and depths (symbols). The most influential taxa (arrows) revealed by SIMPER analysis are Ascidiacea (Asc), Bryozoa (Bry), Cirripedia (Cir), and Echinoidea (Ech). The orientation and length of the arrows represents to which principal component (PC) the taxon contributes the most and how strong. The ellipses depict the 95% confidence interval for each year.

4 Discussion

4.1 Summary of Results

Not all trends in abundance, biomass, and taxonomic composition of seaweed-associated fauna observed between 1996/98 and 2012/13 continued in the same direction until 2021. In 2021, total abundance (i.e., averaged across all depths) doubled compared to 2012, returning to a similar level as in 1996/98. The increase in abundance was accompanied with a shift of peak abundance from 5 m depth in both 1996/98 and 2012 to 10 m in 2021. In 2021, total biomass almost doubled compared to both previous studies and peak biomass shifted to 5 m depth while biomass peaked at 2.5 m in 2013 and 15 m in 1996/98, respectively. In 1996/98, taxonomic composition was distinctly different from the other sampling years, mostly due to a strong increase in cirripedian biomass and decrease in bryozoan biomass. Taxonomic composition also varied along the depth gradient, with bryozoans predominantly found at shallow and cirripedians at greater depths.

4.2 Seaweed as ecosystem engineer

As expected, differences in abundance, biomass and taxonomic composition of seaweed-associated fauna were found throughout the study period. In 2021, total faunal abundance and biomass were higher than in 1996/98 as well as 2013, while total kelp biomass was lower in 2021 compared to 2012/13 (Düsedau et al., 2021). Algal and faunal biomass would be expected to be positively correlated, since seaweeds facilitate associated fauna by increasing habitat complexity, reducing environmental stress, or offering shelter from predation (Ørberg et al., 2018; Wright et al., 2014). Faunal abundance is shown to be increasing with habitat size created by macroalgae and can exceed 100 000 ind. m⁻² in macroalgae beds (Christie et al., 2009). However, seaweeds may also have negative effects on some taxa, such as Cirripedia (Hawkins, 1983), which will be discussed further in chapter 4.4. Cirripedian biomass increased from 22.0% of total biomass in 2012/13 to 51.6% in 2021. Such an increase would be expected to be correlated with a decrease in macroalgal biomass, if macroalgae have a negative impact on cirripedians.

Macroalgal growth in polar areas was predicted to increase due to reductions of sea ice cover and consequently more annual light reaching coastal seafloors (Clark et al., 2013). As the

study site is ice-free since 2006, even in winter (Pavlova et al., 2019), algal biomass would be expected to increase. Total algal biomass did indeed increase between 1996/98 and 2012/13 (Bartsch et al., 2016). The subsequent decrease of kelp biomass in 2021 could be a result of higher water turbidity attenuating underwater irradiance. Higher turbidity may also be one possible explanation for a more shallow vertical distribution limit of most dominant kelp species in Kongsfjorden (Bartsch et al., 2016). Svalbard fjords are likely to become more turbid due to sediment input from increasing glacier melt and coastal run-off caused by global warming (Hanssen-Bauer et al., 2019). Even though increasing growth and biomass of macroalgae was observed throughout the Arctic, locally, e.g. in areas exposed to glacial discharge, algal growth can be reduced (Krause-Jensen et al., 2020). This might also be the case for macroalgae at Hansneset, which are likely influenced by the discharge of Blomstrandbreen, a tidewater glacier located about 5 km northeast of Hansneset (Fig. 1 B).

4.3 Disturbance through ice scouring

In 2021, the strongest increase in biomass of seaweed-associated fauna was found at 5 m depth and below. In addition, faunal abundance peak shifted from 5 m in previous years to 2.5 m depth in 2021. In 2012/13, faunal biomass seemed to match the depth distribution of algal biomass, as peak biomass of both macroalgae and associated fauna shifted to 2.5 m depth in 2012/13, compared to 5 m for macroalgae and 15 m for associated fauna, respectively, in 1996/98. This upwards shift was attributed to a reduction in physical disturbance through ice scour due to major sea ice loss between the first two sampling campaigns (Bartsch et al., 2016; Paar et al., 2016). Despite the lack of sea ice since 2006, ice scouring can still occur through icebergs released by tidewater glaciers. A warmer environment leads to an increased production of icebergs (Błaszczuk et al., 2009). Therefore, more icebergs might be found in Svalbard fjords until the glacier fronts retreat onto land. An increased calving rate has been recorded for Kronebreen, a glacier at the head of Kongsfjorden (Nuth et al., 2012). Additionally, variance within faunal abundance and biomass samples has increased throughout the study period, which might hint at increased disturbance. Since icebergs plough a ridge in the seafloor, while leaving surrounding areas unscathed, different successional stages may exist in a relatively small area, hence increasing variance in benthic assemblages. While icebergs can reach down to 40 m depth in Kongsfjorden, scouring frequency decreases with depth (Dowdeswell & Forsberg, 1992). A less disturbed environment at greater depths might explain the strongest

increase of faunal abundance and biomass at deeper areas, since abundance of sessile biota has been shown to increase with habitat stability (Shunatova et al., 2018)

4.4 Changes in taxonomic composition

Matching the hypothesis, taxonomic composition was more similar between 2021 and 2012/13 than between 2012/13 and 1996/98. The changes in taxonomic composition between 1996/98 and 2012/13 are likely related to the strong increase in algal biomass in the same time period (Bartsch et al., 2016). The increase in algal biomass was attributed to the drastic loss of sea ice in 2006 (Pavlova et al., 2019), reducing ice scouring and extending the open-water period. Paar et al. (2016) found leaf area of brown algae influencing taxonomic composition. Therefore, changes in taxonomic composition between 1996/98 and 2012/13 likely have been caused by the increase in macroalgal biomass. Reduction in kelp biomass observed between 2012/13 and 2021 (Düsedau et al., 2021), seemed to not be sufficient to cause shifts in the taxonomic composition of seaweed-associated fauna, since no significant difference in taxonomic composition was found between 2012/13 and 2021.

Clark et al. (2013) suggested increasing macroalgae growth in polar areas would replace invertebrate communities and reduce coastal biodiversity. As ecosystem engineers, macroalgae modify habitat availability and habitat properties, such as water flow, sedimentation, and irradiance (Layton et al., 2019). These changes in the environment are expected to have a strong impact on benthic communities. An increased algal cover might negatively affect some invertebrate groups, while seaweed-associated fauna should be favoured. Some species, such as the anemone *Caryophyllia smithii*, and the sedentary polychaete *Terebella lapidaria*, were found to be more abundant under low canopy availability (Bustamante et al., 2017). Meanwhile, other species may be facilitated through macroalgae, for instance, shading by the green algae *Ulvopsis grevillei* increases the settlement area suitable for fouling organisms sensitive to UV radiation (Molis et al., 2003). A varied response to algal growth matches the recorded changes in taxonomic composition of benthic fauna related to increased algal growth. In Smeerenburgfjorden, for instance, changes in species composition of benthic fauna were recorded after a large increase of macroalgae cover, mainly by red algae (Al-Habahbeh et al., 2020). While hydrozoan and sponge cover decreased, a simultaneous increase in biomass of seaweed-associated fauna, such as bryozoan and *Spirorbis spirorbis* cover was observed. A reduction of biodiversity in the benthic

ecosystem because of macroalgae growth would not be expected, as some taxa benefit from the new habitat, as described above. Kelps are shown to increase biodiversity not only of associated invertebrates but also of fishes (Miller et al., 2018; Shelamoff et al., 2020). In Hornsund, a three-fold increase in macroalgal biomass resulted in a two-fold increase in the number of benthic species (Weslawski et al., 2010). Hard-bottom benthos in Kongsfjorden was dominated by calcareous red algae, sea urchins and sea anemones until a sudden five-fold increase in macroalgae cover in 1995, just one year before the first sampling for this study. After the increase in macroalgal cover, higher diversity of macrofauna was recorded (Kortsch et al., 2012).

Due to slow growth rates of Arctic species (Barnes & Conlan, 2007), seaweed-associated fauna might need several years to fully adapt to this change in habitat. In Kongsfjorden, the benthic hard bottom community in Kongsfjorden needed about 12 years to recover after a disturbance (Beuchel & Gulliksen, 2008). In Smeerenburgfjorden, a response to an increase in algal cover was observed within 5 years for some species, such as increased *S. spirorbis* abundance or bryozoan *Dendrobeatia* spp. cover. However, a strong increase in abundance of chitons (i.e. *Tonicella* spp.) or the barnacle *Balanus balanus* was seen within 15 years after the abrupt increase in macroalgae cover (Al-Habahbeh et al., 2020). While taxonomic composition changed significantly between 1996/98 and 2012/13, there was little difference in taxonomic composition of seaweed-associated fauna between 2012/13 and 2021. Meanwhile, faunal abundance and biomass increased about two-fold between 2012/13 and 2021. Thus, seaweed-associated fauna might have settled in a new stable state with higher productivity within about 25 years after macroalgae started to dominate hard bottom benthos in Kongsfjorden (Kortsch et al., 2012).

4.4.1 Contrary trends in suspension feeder biomass

The difference of taxonomic composition of seaweed-associated fauna between 1996/98 and the other sampling years was mainly driven by an increase in cirripedian and decrease in bryozoan biomass. Beuchel et al. (2006) also reported major increases in cirripedian *Balanus* sp. abundance in Kongsfjorden in the study period of 1980 - 2003. Al-Habahbeh et al. (2020) found a large increase in both *B. balanus* abundance and bryozoan *Dendrobeatia* spp cover in Smeerenburgfjorden.

Between 2012/13 and 2021, cirripedian biomass increased from 22,0% of total faunal biomass to 51,6%, while total kelp biomass decreased. Even though biomass of the dominating digitate kelps decreased greatly, biomass of *Alaria esculenta* increased (Düsedau et al., 2021). The holdfast of *A. esculenta* seemed to be smaller than holdfasts of digitate kelps (personal observation). Ronowicz et al. (2018) found significant differences between the size of kelp holdfasts, which are likely related to the age of the kelps. Since *A. esculenta* biomass increased since 2012/13, a high percentage of young individuals would be expected. A reduction in number and size of holdfasts possibly opens up primary substrate for cirripedian larvae to settle. Seaweeds seem to have negative effects on settlement of barnacles, not only by limiting substrate availability, but also by sweeping of algal flocs physically removing newly settled barnacles (Jenkins et al., 1999). Moreover, kelps may shade understory algae that compete with sessile invertebrates for space (Miller et al., 2018). At Hansneset, there was a strong decrease of annual macroalgae at 2.5 m and 5 m depth between 1996/98 and 2012/13 (Bartsch et al., 2016). The decline in understory algae might have reduced competition for Cirripedia resulting in the increased cirripedian biomass.

Cirripedia biomass also increased at greater depth. Therefore, other factors, such as food supply, may play an additional role in the increase of cirripedian biomass. As Cirripedia feed on phytoplankton (Kuklinski et al., 2013), positive trends in phytoplankton availability should benefit Cirripedia. Lack of sea ice and related increase in light availability would be expected to benefit phytoplankton, however the opposite effect was observed (Hegseth et al., 2019). Another important food source for benthic suspension feeders is macroalgal detritus, which seems to contribute to about half of cirripedian diet (Renaud et al., 2015)

Contrary to cirripedian biomass, bryozoan biomass decreased from 32.4% of total biomass in 1996/98 to 3,9% in 2021. Bryozoa might be affected by the increasing sediment input into Svalbard fjords through glacier melt and terrestrial run-off (Hanssen-Bauer et al., 2019). Suspension feeders, including bryozoans, were found to prefer areas that are less influenced by glacier discharge (Maughan, 2001; Medelytė et al., 2022). Sedimentation may negatively affect suspension feeders through clogging of the feeding apparatus or inorganic particles diluting food items (Eggleston, 1972; Kuklinski et al., 2005). In 1996/98, bryozoan biomass was ubiquitously distributed across all depths. In 2012/13, Bryozoa were recorded primarily at 2.5 m depth. In 2021, bryozoan biomass declined, but peak bryozoan biomass was still at 2.5 m depth. The shift into shallow waters could be explained by increased sedimentation. The water flow velocity is higher in shallow depths decreasing sedimentation rates and

simultaneously increasing food supply (Kuklinski et al., 2005; Paar et al., 2016). Therefore, shallow waters seem to be a more suitable environment for bryozoan colonies, where bryozoans can longer tolerate the increasing sediment input into the fjord. Voronkov et al. (2013) found biomass of both Bryozoa and Cirripedia decreasing towards the tidal glaciers in inner Kongsfjorden. However, Cirripedia do not seem to be affected by current sedimentation rates at Hansneset, since cirripedian biomass increased throughout the study period. Cirripedia might be more resilient due to their body size, with a larger feeding apparatus not getting clogged by sediment as easily. Maughan (2001) also observed some species, such as *Anomia ephippium*, being less affected by high sedimentation rates than others.

4.5 Food web interactions

The observed increase in faunal biomass might have positive impacts on higher trophic levels, such as fishes or birds, which feed on benthic invertebrates (Fredriksen, 2003). Suspension feeders, such as Cirripedia, usually are primary consumers that feed directly on phytodetritus (Kędra et al., 2012). Detrital food sources are important in polar regions, especially during the winter months, since detritus poses an alternative food source to the seasonal phytoplankton blooms (Norkko et al., 2007). Energy from phytodetritus can be transferred to higher trophic levels through Cirripedia, which predators consists of Gastropoda, such as *Boreotrophon* (Yakovis & Artemieva, 2015). Matching this, biomass of both Cirripedia and Mollusca increased at Hansneset in 2021. Gastropods in return might be eaten by birds, like common eider, or by seals (Hjelset et al., 1999; Kristjánsson et al., 2013). While the increase in faunal biomass is expected to have positive effects on higher trophic levels, changes in taxa composition might cause varied responses. Predators often show preferences for specific prey (Eloranta et al., 2013). A decrease in the abundance of a specific prey item might negatively affect the predator, even if total biomass is increasing at lower trophic levels. Therefore, it is difficult to predict changes within complex food webs.

4.6 Future outlook

Kelp forests are predicted to expand in the Arctic with warming temperatures, providing new habitat for associated fauna (Krause-Jensen & Duarte, 2014). At the same time, the distribution limit of temperate species may shift northwards altering species composition

(Filbee-Dexter et al., 2019). Changes in algal species composition likely impact species composition and abundance of associated fauna. Lippert et al. (2001) found thallus morphology of macroalgae to influence composition of associated fauna in Kongsfjorden. For instance, the kelps *Laminaria digitata* and *Alaria esculenta* were dominated by the bryozoan *Celleporella hyalina*, while the red algae *Phycodrys rubens* was dominated by the polychaete *Spirorbis* aff. *spirillum*. Not only species composition, but also abundance and biomass of seaweed-associated fauna might be affected by the algal species composition. *Laminaria hyperborea* seemed to be a preferred substrate for settlement to *L. digitata* (Schultze et al., 1990). In the north-east Atlantic, warm-temperate kelp species are expanding their distribution range where they support higher density of invertebrate grazers compared to a cold-temperate species (Pessarrodona et al., 2019). In the future, Atlantic macroalgae species might expand their distribution range to Svalbard due to borealization, which would have profound consequences for associated fauna. Moreover, other environmental factors not discussed in this thesis, such as direct temperature impact, salinity or pH, will change in the future (Hanssen-Bauer et al., 2019) and likely alter species composition and abundance in Arctic ecosystems.

4.7 Conclusion

Changes in abundance, biomass, and taxonomic composition of seaweed-associated fauna were found across the study period and the depth gradient. Taxonomic composition seemed to be more similar between 2021 and 2012/13 than between 2012/13 and 1996/98, matching the hypothesis. However, both abundance and biomass increased about two-fold. This might indicate a new stable state with higher productivity of seaweed-associated fauna. The difference in taxonomic composition of seaweed-associated fauna between 2021 and 1996/98 was mainly a result of an increase in cirripedian biomass and a decrease in bryozoan biomass. Different taxa might have varied responses to biotic factors, such as algae cover, and abiotic factors, such as sedimentation. The observed changes in abundance, biomass and taxonomic composition might have cascading effects on the benthic food web in Kongsfjorden. Further changes in Arctic kelp forest can be expected in the future due to continues warming.

References

- Aas, K. S., Dunse, T., Collier, E., Schuler, T. V., Berntsen, T. K., Kohler, J., & Luks, B. (2016). The climatic mass balance of Svalbard glaciers: a 10-year simulation with a coupled atmosphere–glacier mass balance model. *The Cryosphere*, *10*(3), 1089–1104. <https://doi.org/10.5194/tc-10-1089-2016>
- Abdi, H., & Williams, L. J. (2010). Principal component analysis. *Wiley interdisciplinary reviews: computational statistics*, *2*(4), 433–459. <https://doi.org/10.1002/wics.101>
- Al-Hababeh, A. K., Kortsch, S., Bluhm, B. A., Beuchel, F., Gulliksen, B., Ballantine, C., Cristini, D., & Primicerio, R. (2020). Arctic coastal benthos long-term responses to perturbations under climate warming. *Philosophical Transactions of the Royal Society A: Mathematical, Physical and Engineering Sciences*, *378*(2181), 20190355. <https://doi.org/10.1098/rsta.2019.0355>
- Anderson, M. J. (2017). Permutational Multivariate Analysis of Variance (PERMANOVA). *Wiley StatsRef: Statistics Reference Online*, 1–15. <https://doi.org/10.1002/9781118445112.stat07841>
- Barnes, D. K. A., & Conlan, K. E. (2007). Disturbance, colonization and development of Antarctic benthic communities. *Philosophical Transactions of the Royal Society B: Biological Sciences*, *362*(1477), 11–38. <https://doi.org/10.1098/rstb.2006.1951>
- Bartsch, I., Paar, M., Fredriksen, S., Schwanitz, M., Daniel, C., Hop, H., & Wiencke, C. (2016). Changes in kelp forest biomass and depth distribution in Kongsfjorden, Svalbard, between 1996–1998 and 2012–2014 reflect Arctic warming. *Polar Biology*, *39*, 2021–2036. <https://doi.org/10.1007/s00300-015-1870-1>
- Berge, J., Johnsen, G., Nilsen, F., Gulliksen, B., & Slagstad, D. (2005). Ocean temperature oscillations enable reappearance of blue mussels *Mytilus edulis* in Svalbard after a 1000 year absence. *Marine Ecology Progress Series*, *303*, 167–175. <https://doi.org/10.3354/meps303167>
- Beuchel, F., & Gulliksen, B. (2008). Temporal patterns of benthic community development in an Arctic fjord (Kongsfjorden, Svalbard): results of a 24-year manipulation study. *Polar Biology*, *31*(8), 913–924. <https://doi.org/10.1007/s00300-008-0429-9>
- Beuchel, F., Gulliksen, B., & Carroll, M. L. (2006). Long-term patterns of rocky bottom macrobenthic community structure in an Arctic fjord (Kongsfjorden, Svalbard) in relation to climate variability (1980–2003). *Journal of Marine Systems*, *63*(1), 35–48. <https://doi.org/10.1016/j.jmarsys.2006.05.002>
- Bischof, K., Hanelt, D., TuÈg, H., Karsten, U., Brouwer, P. E., & Wiencke, C. (1998). Acclimation of brown algal photosynthesis to ultraviolet radiation in Arctic coastal waters (Spitsbergen, Norway). *Polar Biology*, *20*(6), 388–395. <https://doi.org/10.1007/s0030000050319>
- Błaszczuk, M., Jania, J. A., & Hagen, J. O. (2009). Tidewater glaciers of Svalbard: Recent changes and estimates of calving fluxes. *Polish Polar Research*, *30*(2), 85–142.
- Bloshkina, E. V., Pavlov, A. K., & Filchuk, K. (2021). Warming of Atlantic Water in three west Spitsbergen fjords: recent patterns and century-long trends. *Polar research*, *40*. <https://doi.org/10.33265/polar.v40.5392>
- Bracken, M. E. S., Gonzalez-Dorantes, C. A., & Stachowicz, J. J. (2007). Whole-community mutualism: Associated invertebrates facilitate a dominant habitat-forming seaweed. *Ecology*, *88*(9), 2211–2219. <https://doi.org/10.1890/06-0881.1>
- Bruno, J. F., Stachowicz, J. J., & Bertness, M. D. (2003). Inclusion of facilitation into ecological theory. *Trends in ecology & evolution*, *18*(3), 119–125. [https://doi.org/10.1016/S0169-5347\(02\)00045-9](https://doi.org/10.1016/S0169-5347(02)00045-9)

- Bustamante, M., Tajadura, J., Díez, I., & Saiz-Salinas, J. I. (2017). The potential role of habitat-forming seaweeds in modeling benthic ecosystem properties. *Journal of Sea Research*, 130, 123-133. <https://doi.org/10.1016/j.seares.2017.02.004>
- Charpy-Roubaud, C., & Sournia, A. (1990). The comparative estimation of phytoplanktonic, microphytobenthic and macrophytobenthic primary production in the oceans. *Marine Microbial Food Webs*, 4(1), 31-57.
- Christie, H., Norderhaug, K. M., & Fredriksen, S. (2009). Macrophytes as habitat for fauna. *Marine Ecology Progress Series*, 396, 221-233. <https://doi.org/10.3354/meps08351>
- Clark, G. F., Stark, J. S., Johnston, E. L., Runcie, J. W., Goldsworthy, P. M., Raymond, B., & Riddle, M. J. (2013). Light-driven tipping points in polar ecosystems. *Global Change Biology*, 19(12), 3749-3761. <https://doi.org/10.1111/gcb.12337>
- Clarke, K. R., & Ainsworth, M. (1993). A method of linking multivariate community structure to environmental variables. *Marine Ecology - Progress Series*, 92, 205-219.
- Cottier, F., Tverberg, V., Inall, M., Svendsen, H., Nilsen, F., & Griffiths, C. (2005). Water mass modification in an Arctic fjord through cross - shelf exchange: The seasonal hydrography of Kongsfjorden, Svalbard. *Journal of Geophysical Research: Oceans*, 110(C12005). <https://doi.org/10.1029/2004JC002757>
- Cottier, F. R., Nilsen, F., Inall, M. E., Gerland, S., Tverberg, V., & Svendsen, H. (2007). Wintertime warming of an Arctic shelf in response to large - scale atmospheric circulation. *Geophysical Research Letters*, 34(10). <https://doi.org/10.1029/2007GL029948>
- Durlak, J. A. (2009). How to Select , Calculate , and Interpret Effect Sizes. *Journal of Pediatric Psychology*, 34(9), 917-928. <https://doi.org/10.1093/jpepsy/jsp004>
- Düsedau, L., Fredriksen, S., Brand, M., Savoie, A., Jungblut, S., Molis, M., Niklass, J., Buschbaum, C., Bischof, K., & Bartsch, I. (2021). Macroalgal biodiversity and biomass of Kongsfjorden through time and space. In Oslo: Svalbard Science Conference.
- Eggleston, D. (1972). Factors influencing the distribution of sub-littoral ectoprocts off the south of the Isle of Man (Irish Sea). *Journal of Natural History*, 6(3), 247-260. <https://doi.org/10.1080/00222937200770241>
- Eloranta, A. P., Knudsen, R., & Amundsen, P.-A. (2013). Niche segregation of coexisting Arctic charr (*Salvelinus alpinus*) and brown trout (*Salmo trutta*) constrains food web coupling in subarctic lakes. *Freshwater Biology*, 58(1), 207-221. <https://doi.org/10.1111/fwb.12052>
- Filbee-Dexter, K., Wernberg, T., Fredriksen, S., Norderhaug, K. M., & Pedersen, M. F. (2019). Arctic kelp forests: Diversity, resilience and future. *Global and Planetary Change*, 172, 1-14. <https://doi.org/10.1016/j.gloplacha.2018.09.005>
- Fredriksen, S. (2003). Food web studies in a Norwegian kelp forest based on stable isotope ($\delta^{13}\text{C}$ and $\delta^{15}\text{N}$) analysis. *Marine Ecology Progress Series*, 260, 71-81. <https://doi.org/10.3354/meps260071>
- Fritz, M., Vonk, J. E., & Lantuit, H. (2017). Collapsing Arctic coastlines. *Nature Climate Change*, 7(1), 6-7. <https://doi.org/10.1038/nclimate3188>
- Greenacre, M. (2017). ‘Size’ and ‘shape’ in the measurement of multivariate proximity. *Methods in Ecology and Evolution*, 8, 1415-1424. <https://doi.org/10.1111/2041-210X.12776>
- Hanelt, D., Tüg, H., Bischof, K., Groß, C., Lippert, H., Sawall, T., & Wiencke, C. (2001). Light regime in an Arctic fjord: a study related to stratospheric ozone depletion as a basis for determination of UV effects on algal growth. *Marine Biology*, 138(3), 649-658. <https://doi.org/10.1007/s002270000481>

- Hanssen-Bauer, I., Førland, E. J., Hisdal, H., Mayer, S., Sandø, A. B., & Sorteberg, A. (2019). Climate in Svalbard 2100 – a knowledge base for climate adaptation. NCCS report 1/2019. <https://doi.org/10.25607/OBP-888>
- Hartmann, K., Krois, J., & Waske, B. (2018). *E-Learning Project SOGA: Statistics and Geospatial Data Analysis*. Department of Earth Sciences, Freie Universitaet Berlin. <https://www.geo.fu-berlin.de/en/v/soga/Geodata-analysis/Principal-Component-Analysis/principal-components-basics/Interpretation-and-visualization/index.html>
- Hawkins, S. J. (1983). Interactions of Patella and macroalgae with settling Semibalanus balanoides (L.). *Journal of Experimental Marine Biology and Ecology*, 71(1), 55-72. [https://doi.org/10.1016/0022-0981\(83\)90104-1](https://doi.org/10.1016/0022-0981(83)90104-1)
- Hedges, L. V., Gurevitch, J., & Curtis, P. S. (1999). The meta-analysis of response ratios in experimental ecology. *Ecology*, 80(4), 1150-1156. [https://doi.org/10.1890/0012-9658\(1999\)080\[1150:TMAORR\]2.0.CO;2](https://doi.org/10.1890/0012-9658(1999)080[1150:TMAORR]2.0.CO;2)
- Hegseth, E. N., Assmy, P., Wiktor, J. M., Wiktor, J., Kristiansen, S., Leu, E., Tverberg, V., Gabrielsen, T. M., Skogseth, R., & Cottier, F. (2019). Phytoplankton Seasonal Dynamics in Kongsfjorden, Svalbard and the Adjacent Shelf. In H. Hop & C. Wiencke (Eds.), *The Ecosystem of Kongsfjorden, Svalbard* (pp. 173-227). Springer International Publishing. https://doi.org/10.1007/978-3-319-46425-1_6
- Hjelset, A. M., Andersen, M., Gjertz, I., Lydersen, C., & Gulliksen, B. (1999). Feeding habits of bearded seals (*Erignathus barbatus*) from the Svalbard area, Norway. *Polar Biology*, 21(3), 186-193. <https://doi.org/10.1007/s003000050351>
- Hop, H., Wiencke, C., Vögele, B., & Kovaltchouk, N. A. (2012). Species composition, zonation, and biomass of marine benthic macroalgae in Kongsfjorden, Svalbard. *Botanica Marina*, 55(4), 399-414. <https://doi.org/10.1515/bot-2012-0097>
- Ieno, E. N., & Zuur, A. F. (2015). *A Beginner's guide to data exploration and visualisation with R*. Highland Statistics Limited.
- Isaksen, K., Nordli, Ø., Førland, E. J., Łupikasza, E., Eastwood, S., & Niedźwiedz, T. (2016). Recent warming on Spitsbergen—Influence of atmospheric circulation and sea ice cover. *Journal of Geophysical Research: Atmospheres*, 121(20), 11,913-911,931. <https://doi.org/10.1002/2016JD025606>
- Isaksen, K., Nordli, Ø., Ivanov, B., Køltzow, M. A., Aaboe, S., Gjeltén, H. M., Mezghani, A., Eastwood, S., Førland, E., & Benestad, R. E. (2022). Exceptional warming over the Barents area. *Scientific reports*, 12(1), 1-18. <https://doi.org/10.1038/s41598-022-13568-5>
- Jenkins, S. R., Norton, T. A., & Hawkins, S. J. (1999). Settlement and post-settlement interactions between Semibalanus balanoides (L.) (Crustacea: Cirripedia) and three species of furoid canopy algae. *Journal of Experimental Marine Biology and Ecology*, 236(1), 49-67. [https://doi.org/10.1016/S0022-0981\(98\)00189-0](https://doi.org/10.1016/S0022-0981(98)00189-0)
- Kędra, M., Kuliński, K., Walkusz, W., & Legeżyńska, J. (2012). The shallow benthic food web structure in the high Arctic does not follow seasonal changes in the surrounding environment. *Estuarine, Coastal and Shelf Science*, 114, 183-191. <https://doi.org/10.1016/j.ecss.2012.08.015>
- Kortsch, S., Primicerio, R., Beuchel, F., Renaud, P. E., Rodrigues, J., Lønne, O. J., & Gulliksen, B. (2012). Climate-driven regime shifts in Arctic marine benthos. *Proceedings of the National Academy of Sciences*, 109(35), 14052-14057. <https://doi.org/10.1073/pnas.1207509109>
- Krause-Jensen, D., Archambault, P., Assis, J., Bartsch, I., Bischof, K., Filbee-Dexter, K., Dunton, K. H., Maximova, O., Ragnarsdóttir, S. B., Sejr, M. K., Simakova, U., Spiridonov, V., Wegeberg, S., Winding, M. H. S., & Duarte, C. M. (2020). Imprint of

- Climate Change on Pan-Arctic Marine Vegetation. *Frontiers in Marine Science*, 7. <https://doi.org/10.3389/fmars.2020.617324>
- Krause-Jensen, D., & Duarte, C. M. (2014). Expansion of vegetated coastal ecosystems in the future Arctic. *Frontiers in Marine Science*, 1. <https://doi.org/10.3389/fmars.2014.00077>
- Kristjánsson, T. Ö., Jónsson, J. E., & Svavarsson, J. (2013). Spring diet of common eiders (*Somateria mollissima*) in Breiðafjörður, West Iceland, indicates non-bivalve preferences. *Polar Biology*, 36(1), 51-59. <https://doi.org/10.1007/s00300-012-1238-8>
- Kuklinski, P., Berge, J., McFadden, L., Dmoch, K., Zajaczkowski, M., Nygård, H., Piwosz, K., & Tatarek, A. (2013). Seasonality of occurrence and recruitment of Arctic marine benthic invertebrate larvae in relation to environmental variables. *Polar Biology*, 36(4), 549-560. <https://doi.org/10.1007/s00300-012-1283-3>
- Kuklinski, P., Gulliksen, B., Lønne, O. J., & Weslawski, J. M. (2005). Composition of bryozoan assemblages related to depth in Svalbard fjords and sounds. *Polar Biology*, 28(8), 619-630. <https://doi.org/10.1007/s00300-005-0726-5>
- Lajeunesse, M. J. (2011). On the meta-analysis of response ratios for studies with correlated and multi-group designs. *Ecology*, 92(11), 2049-2055. <https://doi.org/10.1890/11-0423.1>
- Layton, C., Shelamoff, V., Cameron, M. J., Tatsumi, M., Wright, J. T., & Johnson, C. R. (2019). Resilience and stability of kelp forests: The importance of patch dynamics and environment-engineer feedbacks. *PLOS ONE*, 14(1), e0210220. <https://doi.org/10.1371/journal.pone.0210220>
- Lippert, H., Iken, K., Rachor, E., & Wiencke, C. (2001). Macrofauna associated with macroalgae in the Kongsfjord (Spitsbergen). *Polar Biology*, 24(7), 512-522. <https://doi.org/10.1007/s003000100250>
- Lobban, C., & Harrison, P. (1994). *Seaweed ecology and physiology*. Cambridge University. <https://doi.org/10.1017/CBO9780511626210.003>
- Martinez Arbizu, P., & Monteux, S. (2017). *Pairwise Multilevel Comparison using Adonis*. (Version 0.4)
- Maturilli, M., Herber, A., & König-Langlo, G. (2013). Climatology and time series of surface meteorology in Ny-Ålesund, Svalbard. *Earth System Science Data*, 5(1), 155-163. <https://doi.org/10.5194/essd-5-155-2013>
- Maughan, B. C. (2001). The effects of sedimentation and light on recruitment and development of a temperate, subtidal, epifaunal community. *Journal of Experimental Marine Biology and Ecology*, 256(1), 59-71. [https://doi.org/10.1016/S0022-0981\(00\)00304-X](https://doi.org/10.1016/S0022-0981(00)00304-X)
- Medelytė, S., Šiaulys, A., Daunys, D., Włodarska-Kowalczyk, M., Węślawski, J. M., & Olenin, S. (2022). Application of underwater imagery for the description of upper sublittoral benthic communities in glaciated and ice-free Arctic fjords. *Polar Biology*. <https://doi.org/10.1007/s00300-022-03096-3>
- Miller, R. J., Lafferty, K. D., Lamy, T., Kui, L., Rassweiler, A., & Reed, D. C. (2018). Giant kelp, *Macrocystis pyrifera*, increases faunal diversity through physical engineering. *Proceedings of the Royal Society B: Biological Sciences*, 285(1874), 20172571. <https://doi.org/10.1098/rspb.2017.2571>
- Molis, M., Beuchel, F., Laudien, J., Włodarska-Kowalczyk, M., & Buschbaum, C. (2019). Ecological Drivers of and Responses by Arctic Benthic Communities, with an Emphasis on Kongsfjorden, Svalbard. In H. Hop & C. Wiencke (Eds.), *The Ecosystem of Kongsfjorden, Svalbard* (pp. 423-481). Springer International Publishing. https://doi.org/10.1007/978-3-319-46425-1_11

- Molis, M., Lenz, M., & Wahl, M. (2003). Radiation effects along a UV-B gradient on species composition and diversity of a shallow-water macrobenthic community in the western Baltic. *Marine Ecology Progress Series*, 263, 113-125. <https://doi.org/10.3354/meps263113>
- Muckenhuber, S., Nilsen, F., Korosov, A., & Sandven, S. (2016). Sea ice cover in Isfjorden and Hornsund, Svalbard (2000–2014) from remote sensing data. *The Cryosphere*, 10(1), 149-158. <https://doi.org/10.5194/tc-10-149-2016>
- Norderhaug, K. M., Christie, H., & Rinde, E. (2002). Colonisation of kelp imitations by epiphyte and holdfast fauna; a study of mobility patterns. *Marine Biology*, 141(5), 965-973. <https://doi.org/10.1007/s00227-002-0893-7>
- Norderhaug, K. M., Fredriksen, S., & Nygaard, K. (2003). Trophic importance of *Laminaria hyperborea* to kelp forest consumers and the importance of bacterial degradation to food quality. *Marine Ecology Progress Series*, 255, 135-144. <https://doi.org/10.3354/meps255135>
- Norkko, A., Thrush, S. F., Cummings, V. J., Gibbs, M. M., Andrew, N. L., Norkko, J., & Schwarz, A. M. (2007). Trophic structure of coastal Antarctic food webs associated with changes in sea ice and food supply. *Ecology*, 88(11), 2810-2820. <https://doi.org/10.1890/06-1396.1>
- Notz, D., & Stroeve, J. (2016). Observed Arctic sea-ice loss directly follows anthropogenic CO₂ emission. *Science*, 354(6313), 747-750. <https://doi.org/10.1126/science.aag2345>
- Nuth, C., Schuler, T. V., Kohler, J., Altena, B., & Hagen, J. O. (2012). Estimating the long-term calving flux of Kronebreen, Svalbard, from geodetic elevation changes and mass-balance modeling. *Journal of Glaciology*, 58(207), 119-133. <https://doi.org/10.3189/2012JoG11J036>
- Oksanen, J., Blanchet, F. G., Friendly, M., Kindt, R., Legendre, P., McGlinn, D., Minchin, P. R., O'Hara, R. B., Simpson, G. L., Solymos, P., Stevens, M. H. H., Szoecs, E., & Wagner, H. (2020). *Community Ecology Package*. (Version 2.5-7)
- Onarheim, I. H., Eldevik, T., Smedsrud, L. H., & Stroeve, J. C. (2018). Seasonal and regional manifestation of Arctic sea ice loss. *Journal of Climate*, 31(12), 4917-4932. <https://doi.org/10.1175/JCLI-D-17-0427.1>
- Ørberg, S. B., Krause-Jensen, D., Mouritsen, K. N., Olesen, B., Marbà, N., Larsen, M. H., Blicher, M. E., & Sejr, M. K. (2018). Canopy-Forming Macroalgae Facilitate Recolonization of Sub-Arctic Intertidal Fauna and Reduce Temperature Extremes. *Frontiers in Marine Science*, 5. <https://doi.org/10.3389/fmars.2018.00332>
- Orr, E., Hansen, G., Lappalainen, H., Hübner, C., & Lihavainen, H. (2019). SESS report 2018. *Svalbard Integrated Arctic Earth Observing System, Longyearbyen*.
- Paar, M., Voronkov, A., Hop, H., Brey, T., Bartsch, I., Schwanitz, M., Wiencke, C., Lebreton, B., Asmus, R., & Asmus, H. (2016). Temporal shift in biomass and production of macrozoobenthos in the macroalgal belt at Hansneset, Kongsfjorden, after 15 years. *Polar Biology*, 39, 2065-2076. <https://doi.org/10.1007/s00300-015-1760-6>
- Pavlova, O., Gerland, S., & Hop, H. (2019). Changes in Sea-Ice Extent and Thickness in Kongsfjorden, Svalbard (2003–2016). In H. Hop & C. Wiencke (Eds.), *The Ecosystem of Kongsfjorden, Svalbard* (pp. 105-136). Springer, Cham. https://doi.org/10.1007/978-3-319-46425-1_4
- Pessarrodona, A., Foggo, A., & Smale, D. A. (2019). Can ecosystem functioning be maintained despite climate-driven shifts in species composition? Insights from novel marine forests. *Journal of Ecology*, 107(1), 91-104. <https://doi.org/10.1111/1365-2745.13053>
- Polyakov, I. V., Alkire, M. B., Bluhm, B. A., Brown, K. A., Carmack, E. C., Chierici, M., Danielson, S. L., Ellingsen, I., Ershova, E. A., Gårdfeldt, K., Ingvaldsen, R. B.,

- Pnyushkov, A. V., Slagstad, D., & Wassmann, P. (2020). Borealization of the Arctic Ocean in Response to Anomalous Advection From Sub-Arctic Seas [Original Research]. *Frontiers in Marine Science*, 7. <https://doi.org/10.3389/fmars.2020.00491>
- Poore, A. G. B., Campbell, A. H., Coleman, R. A., Edgar, G. J., Jormalainen, V., Reynolds, P. L., Sotka, E. E., Stachowicz, J. J., Taylor, R. B., Vanderklift, M. A., & Emmett Duffy, J. (2012). Global patterns in the impact of marine herbivores on benthic primary producers. *Ecology Letters*, 15(8), 912-922. <https://doi.org/10.1111/j.1461-0248.2012.01804.x>
- R Core Team and contributors worldwide (2021). *The R Stats Package*. (Version 4.1.2)
- Renaud, P. E., Løkken, T. S., Jørgensen, L. L., Berge, J., & Johnson, B. J. (2015). Macroalgal detritus and food-web subsidies along an Arctic fjord depth-gradient [Original Research]. *Frontiers in Marine Science*, 2. <https://doi.org/10.3389/fmars.2015.00031>
- Ronowicz, M., Kukliński, P., & Włodarska-Kowalczyk, M. (2018). Diversity of kelp holdfast-associated fauna in an Arctic fjord - inconsistent responses to glacial mineral sedimentation across different taxa. *Estuarine, Coastal and Shelf Science*, 205, 100-109. <https://doi.org/10.1016/j.ecss.2018.01.024>
- RStudio Team (2021). *RStudio: Integrated Development for R*. (Version 2021.09.1) <http://www.rstudio.com/>
- Scherrer, K. J. N., Kortsch, S., Varpe, Ø., Weyhenmeyer, G. A., Gulliksen, B., & Primicerio, R. (2019). Mechanistic model identifies increasing light availability due to sea ice reductions as cause for increasing macroalgae cover in the Arctic. *Limnology and Oceanography*, 64(1), 330-341. <https://doi.org/10.1002/lno.11043>
- Schuler, T. V., Kohler, J., Elagina, N., Hagen, J. O. M., Hodson, A. J., Jania, J. A., Kääh, A. M., Luks, B., Małeck, J., & Moholdt, G. (2020). Reconciling Svalbard glacier mass balance. *Frontiers in Earth Science*, 8, 156. <https://doi.org/10.3389/feart.2020.00156>
- Schultze, K., Janke, K., Krüß, A., & Weidemann, W. (1990). The macrofauna and macroflora associated with *Laminaria digitata* and *L. hyperborea* at the island of Helgoland (German Bight, North Sea). *Helgoländer Meeresuntersuchungen*, 44(1), 39-51. <https://doi.org/10.1007/BF02365430>
- Shaw, R. G., & Mitchell-Olds, T. (1993). ANOVA for unbalanced data: an overview. *Ecology*, 74(6), 1638-1645. <https://doi.org/10.2307/1939922>
- Shelamoff, V., Layton, C., Tatsumi, M., Cameron, M. J., Wright, J. J. T., Edgar, G. J., & Johnson, C. R. (2020). High kelp density attracts fishes except for recruiting cryptobenthic species. *Marine Environmental Research*, 161, 105127. <https://doi.org/10.1016/j.marenvres.2020.105127>
- Shunatova, N., Nikishina, D., Ivanov, M., Berge, J., Renaud, P. E., Ivanova, T., & Granovitch, A. (2018). The longer the better: the effect of substrate on sessile biota in Arctic kelp forests. *Polar Biology*, 41(5), 993-1011. <https://doi.org/10.1007/s00300-018-2263-z>
- Skålin, R., Jensen, I. S., & Eriksen, T. G. (2022). *Historic Weather Data for Ny-Ålesund*. Norwegian Meteorological Institute, NRK. <https://www.yr.no/nb/historikk/graf/1-2837778/Norge/Svalbard/Svalbard/Ny-%C3%85lesund?q=2021>
- Sukhanova, I. N., Flint, M. V., Pautova, L. A., Stockwell, D. A., Grebmeier, J. M., & Sergeeva, V. M. (2009). Phytoplankton of the western Arctic in the spring and summer of 2002: Structure and seasonal changes. *Deep Sea Research Part II: Topical Studies in Oceanography*, 56(17), 1223-1236. <https://doi.org/10.1016/j.dsr2.2008.12.030>
- Tverberg, V., Skogseth, R., Cottier, F., Sundfjord, A., Walczowski, W., Inall, M. E., Falck, E., Pavlova, O., & Nilsen, F. (2019). The Kongsfjorden transect: seasonal and inter-annual variability in hydrography. In H. Hop & C. Wiencke (Eds.), *The Ecosystem of*

- Kongsfjorden, Svalbard* (pp. 49-104). Springer. <https://doi.org/10.1007/978-3-319-46425-1>
- Viechtbauer, W. (2010). Conducting Meta-Analyses in R with the metafor Package. *Journal of Statistical Software*, 36(3), 1-48. <https://doi.org/10.18637/JSS.V036.I03>
- Voronkov, A., Hop, H., & Gulliksen, B. (2013). Diversity of hard-bottom fauna relative to environmental gradients in Kongsfjorden, Svalbard. *Polar research*, 32(1), 1-27. <https://doi.org/10.3402/polar.v32i0.11208>
- Weslawski, J. M., Wiktor, J., & Kotwicki, L. (2010). Increase in biodiversity in the arctic rocky littoral, Sorkappland, Svalbard, after 20 years of climate warming. *Marine Biodiversity*, 40(2), 123-130. <https://doi.org/10.1007/s12526-010-0038-z>
- Wright, J. T., Byers, J. E., DeVore, J. L., & Sotka, E. E. (2014). Engineering or food? mechanisms of facilitation by a habitat-forming invasive seaweed. *Ecology*, 95(10), 2699-2706. <https://doi.org/10.1890/14-0127.1>
- Yakovis, E., & Artemieva, A. (2015). Bored to Death: Community-Wide Effect of Predation on a Foundation Species in a Low-Disturbance Arctic Subtidal System. *PLOS ONE*, 10(7), e0132973. <https://doi.org/10.1371/journal.pone.0132973>

Appendix

Tab. A1 PERMANOVA results showing the temporal, depth and interactive effect of depth and year on taxonomic composition of seaweed-associated fauna based on abundance data.

Effect	df	Sum of squares	Pseudo-F	R ²	P(perm)
Depth	3	1.44	3.70	0.129	0.003
Year	2	4.26	16.37	0.381	0.000
Depth:Year	6	1.30	1.67	0.117	0.078
Residuals	32	4.16		0.373	
Total	43	11.17		1.000	

Tab. A2 PERMANOVA results showing the temporal, depth and interactive effect of depth and year on taxonomic composition of seaweed-associated fauna based on biomass data.

Effect	df	Sum of squares	Pseudo-F	R ²	P(perm)
Depth	3	2.02	5.66	0.254	0.000
Year	2	1.49	6.25	0.187	0.000
Depth:Year	6	1.12	1.57	0.141	0.060
Residuals	28	3.33		0.419	
Total	39	7.95		1.000	

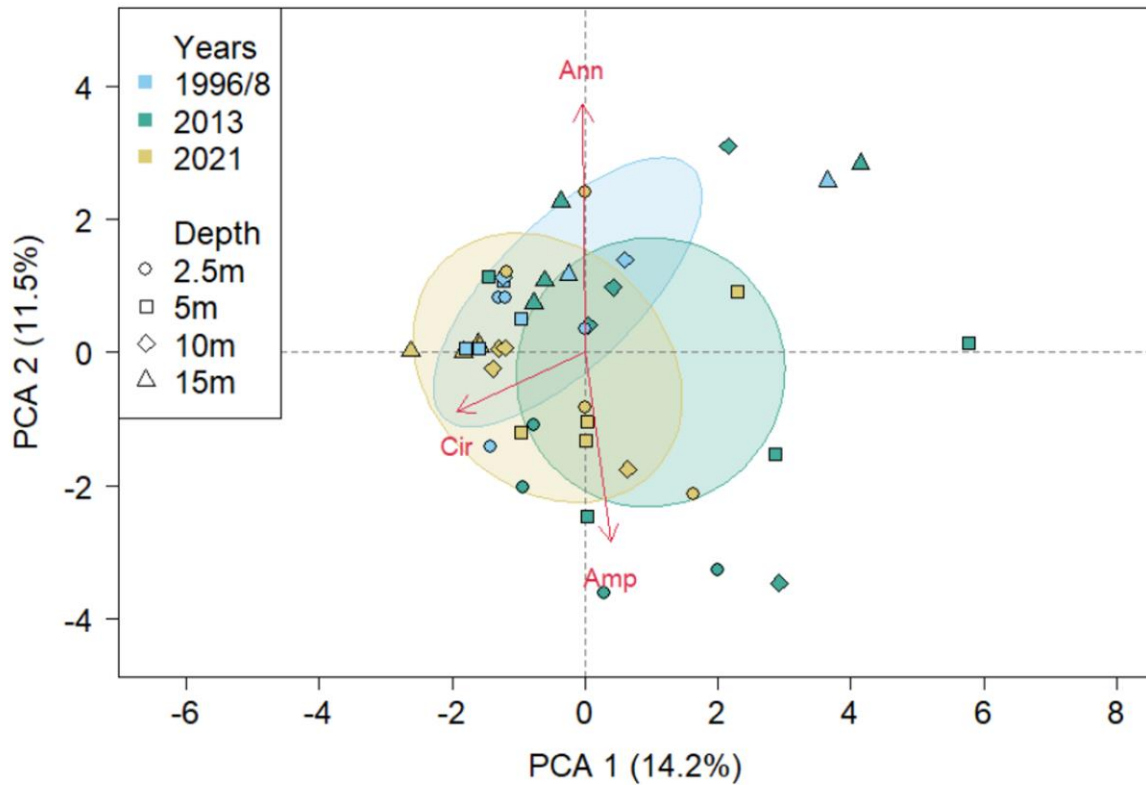


Fig. A1 Principal component analysis based on abundance data showing the difference in taxonomic composition for all combinations of years (color) and depths (symbols). The most influential taxa (arrows) revealed by SIMPER analysis are Annelida (Ann), Amphipoda (Amp), and Cirripedia (Cir). The orientation and length of the arrows represents to which principal component (PC) the taxon contributes the most and how strong. The ellipses depict the 95% confidence interval for each year.

